THE DECAY OF Ta^{183}

Thesis by

Joseph Jackson Murray, Jr.

In Partial Fulfillment of the Requirements

for the Degree of

Doctor of Philosophy

California Institute of Technology

Pasadena, California

1954

ACKNOWLEDGMENTS

The results of this thesis depend on the author's having had at his disposal a gamma and beta spectrometer. The construction and development of these instruments was the work of many, too numerous to mention individually but all under the aegis of Jesse W. M. DuMond. To Dr. DuMond and the others, the author wishes to express his gratitude.

In addition it is a pleasure to acknowledge the contribution of Philip Snelgrove through his efficient operation of the gamma spectrometer and invaluable assistance in the reduction of data therefrom.

The patient guidance and encouragement afforded throughout the experiments by Dr. P. E. Marmier is deeply appreciated.

This work was assisted by the joint program of the Office of Ordnance Research and the Atomic Energy Commission.

ABSTRACT

The β^- decay of Ta^{183} into an excited state of W^{183} has been observed using the curved crystal gamma-ray diffraction spectrometer and the axial focusing homogeneous field beta spectrometer. A unique decay scheme is presented for this mode of excitation of W^{183} constructed on the basis of the energies and conversion properties of twenty-seven gamma transitions with spin and parity assigned to each level. The principal features of the scheme are no parity change throughout, frequent violation of single particle selection rules, and several examples of competition between E2 and M1 transitions. These results provide amplification of and correction to preliminary results reported earlier.[1]

In addition to the primary results above, there will also be found a comparison of the experimental and theoretical K and L conversion coefficients for E2 and M1 transitions in the energy range from 40 to 350 kev and experimental M and N conversion coefficients for a few low energy E2 and M1 transitions.

There is presented a review of the techniques employed and of important parts of the analysis of the experimental data especially with regard to corrections applied to observed intensities of gamma and conversion lines. A brief discussion offers a suggestion for possible interpretation of certain aspects of the results in terms of current ideas about nuclear structure.

---

[1]Dumond, Hoyt, Marmier and Murray, Phys. Rev. 92, 202 (1953).

TABLE OF CONTENTS

I

INTRODUCTION

$_{73}Ta^{183}_{110}$ is an unstable isotope of the heavy metal, tantalum. It is an odd-even nucleus (with an odd number of protons) and should, according to shell theory, have a 7/2+ ground state. It decays, presumably from its ground state, by β^- emission into an excited state of a stable isotope of tungsten, $_{74}W^{183}_{109}$, also odd-even but with an odd number of neutrons. The tungsten nucleus has a 1/2- ground state[1]. Following the β^- decay there is a large number of gammas emitted in the deexicitation of the tungsten nucleus. The β^- decay has a half life of 5.2 days and an end point energy of 615 kev with log (ft) equal[14] to 7.0 indicating (15) a first forbidden $\Delta I=1$, yes transition. The gamma energies extend up to 406 kev with an outstanding line at 246 kev.

The five day activity of tantalum was first observed by Butement [2] in 1950 having been produced by W(n,p) and W(γ,p) reactions and identified chemically. It was tentatively assigned to Ta^{183} at that time. Using these reactions, the half-life, end point energy and 246 kev gamma were also observed by Wilkinson [3] in 1950 and Moses and Martin [4] in 1951.

Observation of the gamma spectrum of Ta^{182} by Hoyt [5] in 1951 showed the presence of an unaccountable short half life activity, that is, much shorter than the 115 day half life of Ta^{182}. The Ta^{182} had been produced by $Ta^{181}(n,\gamma)$

reaction in the Oak Ridge reactor. Shortly afterward it was suggested by Mihelich (6) that this activity was that of Ta^{183} produced by a double neutron capture process, $Ta^{181}(n,\gamma)$ followed by $Ta^{182}(n,\gamma)$. Mihelich looked especially for the short half life activity after irradiation of a Ta^{181} sample in the Brookhaven reactor and indeed found the five day, 615 kev β^- activity and the 246 kev gamma. He estimated the cross section for the second neutron capture in terms of decay fractions of a Ta^{182} gamma and the 246 kev gamma of Ta^{183}. For reasonable values of the decay fractions the result gives 10^4 to 10^5 barns.

The ratio of the populations of Ta^{183} and Ta^{182} produced by the double capture process is proportional to $\sigma_2 \psi/\lambda_3$, where σ_2 is the slow neutron cross section of Ta^{182}, ψ the neutron flux and λ_3 the decay constant of Ta^{183} (see eq. (A3) Appendix I). Hence a high flux yields a larger proportion of Ta^{183}. This advantage was realized in preliminary experiments (7) commenced in May 1953 at California Institute of Technology by employing the Arco reactor* which has a neutron flux roughly 100 times that of the reactor at Brookhaven. An initial activity is obtainable which is almost entirely that of Ta^{183}. Under these conditions it was possible, by comparison of β spectrum intensities of Ta^{182} and Ta^{183}, to set a lower limit on σ_2 of 10^4 barns which is probably not exceeded by more than a factor two. In addition, the preliminary ex-

---

*The efforts of Dr. W. B. Lewis in arranging irradiations in the materials testing reactor at Arco, Idaho are gratefully acknowledged.

periments yielded precision energies for seventeen of the major gamma lines.

This thesis represents the results of a more refined study of the decay of Ta^{183}, commenced in January, 1954, in which the curved crystal gamma spectrometer (5) and the axial focussing homogeneous field beta spectrometer (8) were employed. It is an amplification of and contains a few corrections to the results of the preliminary study. Immediately following will be found a tabular and graphical presentation of the results, the principal item being a proposed decay scheme for this mode of excitation of W^{183} with spin and parity assignments for each level.

Thereafter, the techniques employed and the analysis of certain parts of the experimental data will be reviewed including details of the numerous corrections which were applied to observed gamma and conversion line intensities. Finally, the results will be discussed and, briefly, it will be attempted to relate some of them to current ideas about nuclear structure.

II

RESULTS

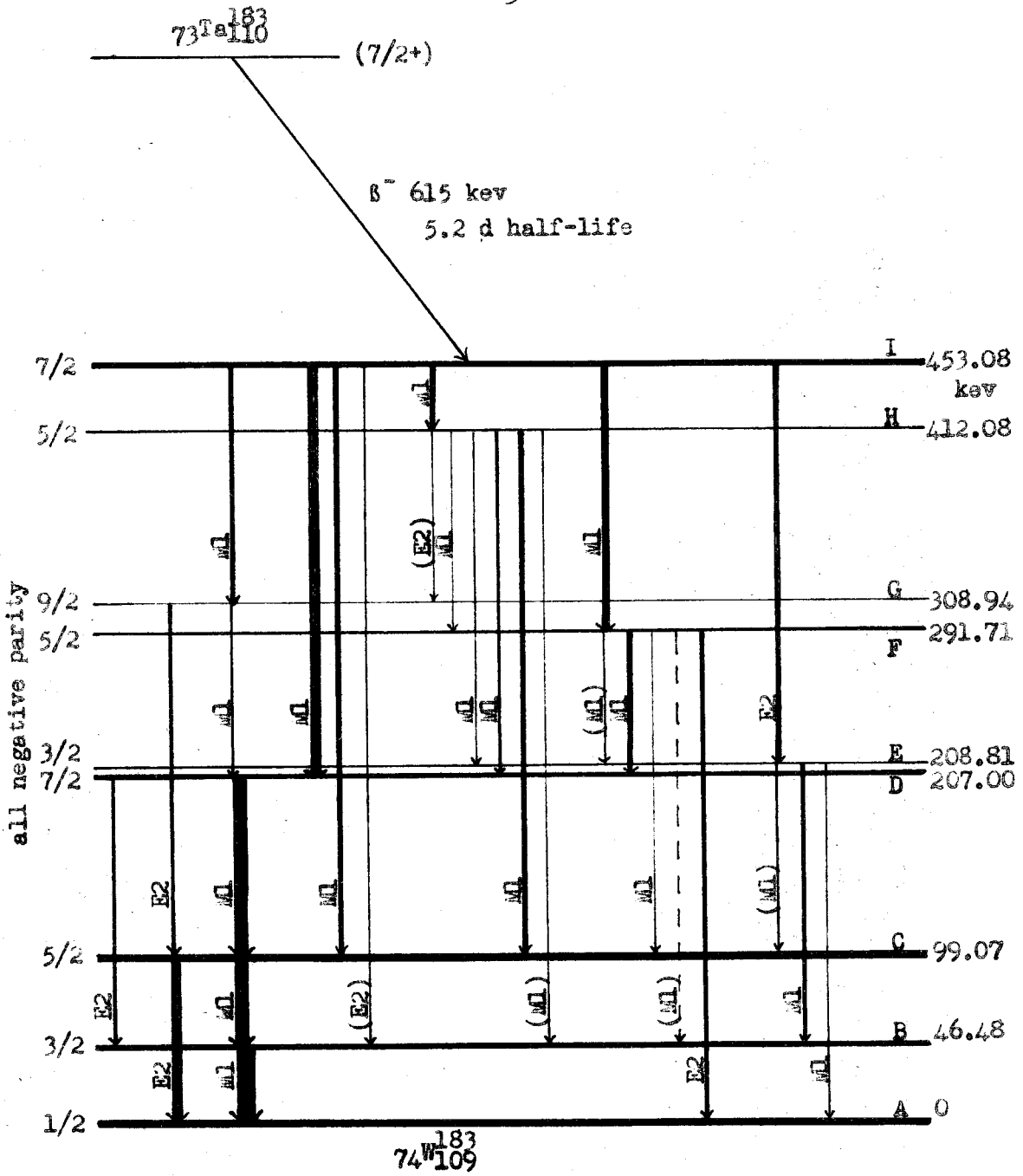

Fig. 1 The ß⁻ decay of Ta^{183} and the decay scheme for W^{183}. Relative excitations of the levels and decay fractions of the transitions are indicated by the weight of the lines. The arrangement of levels is unique as are the spin and parity assignments. Higher energy ß⁻ transitions, if they exist, occur less than 5% as often as the main transition shown. The multipolarities shown in parenthesis were inferred from the diagram . The others were determined by conversion properties of the transitions. Transition FB should exist but was probably obscured by the nearby transitions IE and ID. The other missing transitions would be inferred to have M3 or E4 multipolarities except for HA, GF and ED which would be E2 the latter two of very low energy.

Table 1. Gamma and Conversion Line Characteristics

Initial and final levels	Gamma Lines: Energy kev.	Gamma Lines: Rel. Intens.	Conversion Lines: K Energy kev.	Conversion Lines: K Rel. Intens.	Conversion Lines: L_I Energy kev.	Conversion Lines: L_I Rel. Intens.
IH	40.97±0.01	1.4	-	-	28.87	153±15%
BA	46.48±0.01	13.5	-	-	34.39	950±15%
CB	52.59±0.01	15.0	-	-	40.41	548±10%
FE	82.92±0.01	0.7	-	-	(b)	9.3±15%
FD	84.70±0.02	4.5	-	-	72.58	46±15%
CA	99.07±0.02	13.8	29.56	180±15%	(c)	(11)
GD	101.94±0.02	0.6	32.34	30.5±20%	-	(3.0)
(d)	102.49±0.02	0.25	32.98	82±20%	90.42	15±50%
HG	103.14±0.02	0.2	(e)	(1.4)	-	-
DC	107.93±0.02	23.6	38.32	802±10%	95.70	128±10%
EC	109.73±0.02	1.7	(g)	(51)	(h)	(9)
HF	120.38±0.02	0.3	50.76	3.7	-	(0.9)
(i)	142.25±0.03	1.5	(j)	(15)	130.12	3.0±20%
IG	144.12±0.03	8.5	74.65	84±10%	132.06	14.0±10%
DB	160.53±0.04	10.5	(k)	23±30%	-	(2.2)
IF	161.36±0.04	31.0	91.90	214±10%	(1)	(41)
EB	162.33±0.04	16.5	92.78	111±10%	(1)	(21)
FC	192.64±0.06	0.9	123.21	3.4±20%	-	(0.7)
HE	203.27±0.06	0.9	133.77	3.5±30%	-	(0.6)
HD	205.06±0.06	3.4	135.48	12.2±10%	193.10	2.7±15%
EA	208.81±0.07	2.6	139.23	11.0±15%	(m)	(1.2)
GC	209.87±0.07	16.4	140.24	21.4±15%	-	(1.8)
IE	244.26±0.09	34.0	(n)	30±30%	-	(2)
ID	246.05±0.09	100.0	(r)	228±5%	234.12	42±10%
FA	291.71±0.13	20.0	222.20	8.2±10%	-	-
HC	313.03±0.15	29.0	243.43	38±10%	301.22	6.3±15%
IC	354.04±0.2	42.0	(r)	36±10%	342.08	6.3±15%
HB	365.60±0.2	3.4	(q)	(2.6)	-	-
IB	406.58±0.25	3.8	-	(0.7)	-	-

NOTES:

1. The gamma energies, E, were obtained (by means of the crystal diffraction spectrometer) with a resolution $\frac{\Delta E}{E} = 0.3E \cdot 10^{-2}$ percent where E is gamma energy in kev. The assigned uncertainty is ±1/20 of the resolution or 10 e.v. whichever is larger. The statistical uncertainty was less than half this amount in all cases.

2. The conversion line energies were obtained with a momentum resolution of 0.35%. The assigned uncertainty is ± 1 part in 1000 or 100 e.v., whichever is larger, except where noted.

3. All gamma intensities were at least five times above a level of certain detection. The gamma intensity uncertainty is 20% below 90 kev, 10% elsewhere.

and Identification

L_{II} Energy kev.	L_{II} Rel. Intens.	L_{III} Energy kev.	L_{III} Rel. Intens.	Conversion Coefficient α_K Exp.	α_K Theo.	α_{L_I} Exp.	α_{L_I} Theo.
(a)	(34)	30.77	11±30%	-	-	18.2	11
34.97	141±15%	36.30	64±15%	-	-	11.7	7.3
40.97	126±10%	42.27	79±10%	-	-	6.1	4.8
-	-	-	-	(p)	~7	2.2	1.4
-	-	-	-	(p)	~7	1.7	1.3
87.56	205±10%	88.80	188±10%	2.2	1.3	-	0.13
-	-	-	-	9.3	4.1	-	0.8
-	-	-	-	57	30	10	-
-	(1.5)	-	(1.5)	-	1.2	-	0.13
(f)	(5)	-	-	5.7	3.4	0.9	0.63
-	-	-	-	(5)	3.2	(0.9)	0.61
-	-	-	-	2.1	2.5	-	0.5
-	-	-	-	-	1.55	0.33	0.32
-	(0.9)	-	-	1.65	1.45	0.28	0.30
(1)	(11)	(1)	(9)	0.37	0.29	-	0.035
-	(2.4)	-	-	1.15	1.12	(1)	0.22
-	(1.2)	-	-	1.12	1.10	(1)	0.21
-	-	-	-	0.63	0.72	-	0.13
-	-	-	-	0.65	0.62	-	0.11
-	(0.12)	-	-	0.59	0.61	0.13	0.10
-	(0.08)	-	-	0.70	0.60	-	0.09
198.29	6.5±15%	199.69	3±15%	0.22	0.145	-	0.018
(o)	(6)	(o)	(4)	0.147	0.10	-	0.01
-	(1.5)	-	-	0.38	0.38	0.07	0.06
279.98	2.8±15%	-	-	0.068	0.064	-	0.007
-	-	-	-	0.22	0.20	0.036	0.028
-	-	-	-	0.143	0.145	0.025	0.019
-	-	-	-	-	0.13	-	-
-	-	-	-	-	0.03	-	-

[Letter in parenthesis refers to a note.

4. On the scale of relative conversion line intensities, 1 to 2 represents the level of certain detection under good conditions. Below 50 kev. this value increases in accordance with the reduction in the β counter efficiency (see TECHNIQUE AND ANALYSIS, Conversion Line Intensities).

5. The total conversion coefficient, α_T (experimental), contains M and N conversion coefficients from Table 2 where available. Where only part of the total conversion was observed, α_T contains theoretical values for the unobserved parts.

ficients $\alpha_{L_{II}}$ Exp.	Theo.	$\alpha_{L_{III}}$ Exp.	Theo.	α_T(total) Exp.	Decay Fraction %	Multipole Assignment
(4.0)	1.1	1.3	0.05	29.1	10.3	M1
1.7	0.5	0.8	0.05	17.5	61.4	M1
1.4	0.3	0.9	0.05	10.3	41.7	M1
-	0.07	-	-	(14)	2.5	(M1)
-	0.06	-	-	(13)	14.2	M1
2.5	1.5	2.3	1.4	8.4	31.9	E2
-	-	-	-	10.5	1.55	M1
-	--	-	-	70	4.2	M2
-	1.3	-	1.3	10	0.5	(E2)
-	0.03	-	-	6.9	45.7	M1
-	0.03	-	-	(5.9)	2.9	(M1)
-	-	-	-	2.7	0.25	M1
-	-	-	-	~2.0	1.1	M1
-	0.018	-	-	2.03	6.4	M1
(1)	0.17	(1)	0.14	0.75	4.4	E2
-	0.013	-	-	1.4	18.2	M1
-	0.012	-	-	1.4	9.8	M1
-	-	-	-	0.76	0.4	M1
-	-	-	-	0.76	0.4	M1
-	0.006	-	-	0.72	1.45	M1
-	0.006	-	-	0.81	1.15	M1
0.066	0.055	0.031	0.037	0.34	5.4	E2
-	0.03	-	0.02	0.2	10.0	E2
-	0.002	-	-	0.45	35.6	M1
0.023	0.013	-	0.006	0.09	5.4	E2
-	-	-	-	0.26	8.8	M1
-	-	-	-	0.17	12.0	M1
-	-	-	-	-	0.85	(M1)
-	-	-	-	-	0.95	(E2)

A dash indicates no relevant entry.]

6. Theoretical K conversion coefficients have been interpolated or extrapolated graphically from the calculations of Rose *et al.*[9] Theoretical L conversion coefficients have been obtained similarly from the calculations of Gellman *et al.*[10].

7. The decay fractions were computed using observed values of the total conversion coefficient and are normalized so that the total fraction into the ground state is 100 (see Table 3 also).

Notes for Table 1 (cont):

8. Numbers in parenthesis are expected values not observed. In the case of certain conversion line intensities a small number provides the reason for lack of observation. In other cases a note (indicated by letter) provides an explanation.

9. The absorption edges in kev for the K and L shells in tungsten (converting element) are [22]:

K	69.51	L_{II}	11.54
L_I	12.09	L_{III}	10.20

(a) An observable L_{II} line probably exists but would be almost coincident with the 99.07 kev K line. With an expected intensity on the order of only 5% of that of the K line, its existence could not be verified. The L_{III} line was probably observed although it occurred just above and unresolved with the K line of a 100.02 kev gamma belonging to Ta^{182}. At the time of observation its intensity was only about 20% of the K line's intensity, hence, very uncertain.

(b) An L conversion line of this transition was undoubtedly observed but the energy determination was sufficiently inaccurate so that identification as L_I or L_{II} was not possible. Consequently there was insufficient evidence for making a multipolarity assignment.

(c) An observable L_I line probably exists but would occur just below and unresolved with the much larger L_{II} line so its existence could not be verified.

(d) For reasons explained in the section, TECHNIQUE AND ANALYSIS, subsections, Gamma Energies and Their Role in Construction of the Level Scheme and Multipolarity Assignments and Parity,

Notes for Table 1 (cont):

this transition is not believed to be part of the main scheme, although from its half life it appears to belong to the Ta^{183} decay.

(e) An observable K line may exist but would occur unresolved on the low energy side of the very large L_I line of the 46.48 kev transition. Its existence could not be verified.

(f) An observable L_{II} line probably exists but would occur unresolved with the much larger M_{III} line of the 99.07 kev transition so its existence could not be verified. Furthermore, it was necessary to decompose the same 99.07 kev M_{III} line, just barely resolved, from the 107.93 kev L_I line in order to obtain the energy of the latter. This accounts for the poor energy determination for the L_I line. Nevertheless its identification was definite.

(g) The K line was unresolved with the L_I line of the 52.59 kev transition. An observed broadening of the latter was consistent with the intensity of the K line of the 109.73 kev transition expected on the basis of the theoretical K-conversion coefficient for the M1 multipolarity inferred from the decay scheme. Furthermore, as explained in note (h), the L_I line was not observed at all so there was no sound basis for a multipolarity assignment for this transition.

(h) An observable L_I line probably exists but would be completely unresolved with and much smaller than the M_{III} line of the 100.02 kev transition belonging to Ta^{182}. Its existence could not be verified.

Notes for Table 1 (cont):

(i) For reasons explained in the section, TECHNIQUE AND ANALYSIS, subsection Gamma Energies and Their Role in Construction of the Level Scheme, this transition is not believed to be part of the main scheme, although from its half life it appears to belong to the decay of Ta^{183}.

(j) An observable K line may exist but would occur unresolved with the much larger L_I line of the 84.70 kev transition. Its existence could not be verified. The only evidence for making the multipole assignment, M1, therefore, was identification of the small L_I line.

(k) The K line was undoubtedly observed but was unresolved on the low energy side of the 161.36 kev K line. The intensity could be estimated reasonably well but a good energy determination was not possible. No other conversion lines of comparable intensity were expected in the immediate vicinity so the identification is probably correct.

(l) The L lines of the 160.53, 161.36 and 162.33 kev transitions formed an unresolved group. For a discussion and interpretation of this group of lines see APPENDIX II.

(m) The L_I line may have been observed, unresolved on the low energy side of the L_{II} line of the 209.87 kev transition. Very uncertain. It could also be confused with a small, nearly coincident K line of the 365.60 kev transition.

(n) The K line was very evident though nearly unresolved with the much larger K line of the 246.05 kev transition. The intensity could be estimated reasonably well but a good energy determination was not possible.

Notes for Table 1 (cont):

(o) Observable L_{II} and L_{III} lines almost certainly exist but both were unresolved with the much larger L_I line of the 246.05 kev transition. Their existence could not be verified. If, however, the transition were M1, rather than E2 as assigned, an L_I line would have been expected of sufficient intensity and enough separation from the 246.05 kev L_I line to have been easily observable. There was no evidence for its existence. This negative observation strengthens the E2 assignment.

(p) Theoretical K-conversion coefficients for gamma energies this low are gross extrapolations of actual theoretical calculations [9] which extend only to 150 kev. For this reason and because of the effect of screening, the value obtained from the theoretical curve of Fig. 2 may be in error, probably low by a considerable amount. About twice this "theoretical" value was used in the estimate of α_T listed here. Obviously the estimate for α_T is very uncertain.

(q) The K line may have been observed, unresolved on the low energy side of the L_{II} line of the 209.87 kev transition. Very uncertain. It could also be confused with a small, nearly coincident L_I line of the 208.81 kev transition.

(r) K-conversion lines of 246.05 and 354.04 kev gammas used as calibration lines for conversion energies below and above 250 kev respectively.

Table 2. M and N Shell Conversion Lines and Coefficients

Gamma Line		M Conversion Line			N Conversion Line		
Energy kev.	Intens.	Energy kev.	Intens.	Conv. Coeff.	Energy kev.	Intens.	Conv. Coeff.
40.97	1.4	Note 2	(36)	(4.3)	Note 2	(11)	(1.3)
46.48	13.5	43.67(I)	204	2.5	45.87(I)	60	.74
52.59	15.0	49.85(I)	130	1.45	52.01(I)	37	.41
84.70	4.5	81.82(I)	8.8	.33	-	-	-
99.07	13.8	96.69(III)	94	1.14	98.60(II)	27	.33
107.93	23.6	105.10(I)	34	.24	107.58(I)	9.6	.07
144.12	8.5	141.29(I)	5.0	0.10	-	-	-

NOTES:

1. Roman numerals in parenthesis after conversion line energies indicate shell, identified by the energy, in which conversion took place.
2. M_I line unresolved with K line of 107.93 kev transition. Impossible to estimate intensity. Similarly, N_I line unresolved with L_I line of 52.59 kev transition. Values in parenthesis were estimated on the basis of corresponding values for the 52.59 and 46.48 kev transition. The estimated conversion coefficients were used in evaluation of α_T in Table 1.

(See Fig. 4 for graphical representation of M and N conversion coefficients)

Table 3

Total Decay Fractions into and out of the Levels

(in % of input to ground state A)

Level	Total Decay Fraction	
	in	out
I	-	93.6
H	10.3	12.3
G	6.9	6.9
F	18.4	22.5
E	12.9	13.8
D	52.8	50.1
C	75.2	73.8
B	57.8	61.4
A	100.0	-

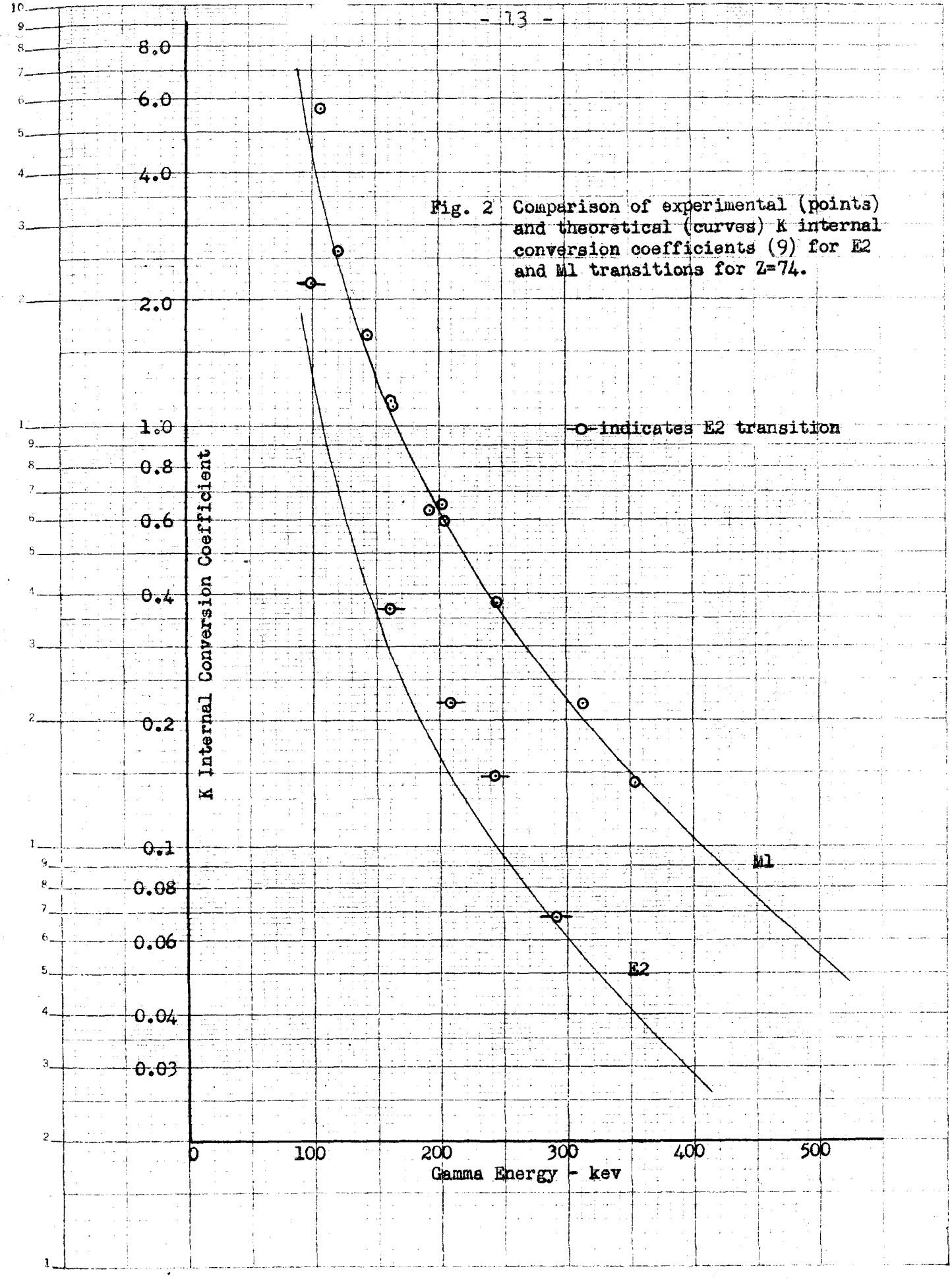

Fig. 2 Comparison of experimental (points) and theoretical (curves) K internal conversion coefficients (9) for E2 and M1 transitions for Z=74.

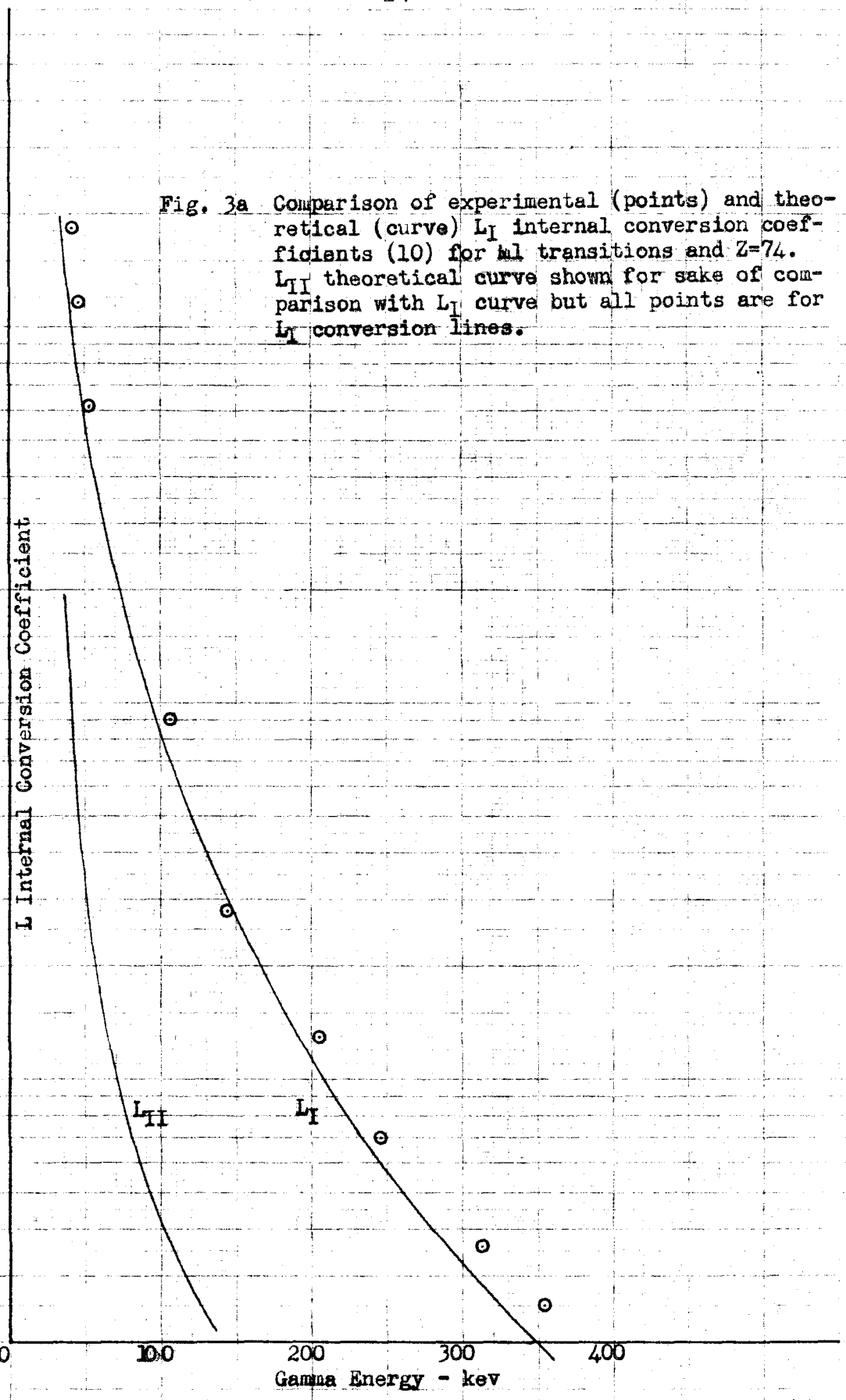

Fig. 3a Comparison of experimental (points) and theoretical (curve) L_I internal conversion coefficients (10) for M1 transitions and Z=74. L_{II} theoretical curve shown for sake of comparison with L_I curve but all points are for L_I conversion lines.

Fig. 3b Comparison of experimental (points) and theoretical (curves) L_{II} and L_{III} internal conversion coefficients (10) for E2 transitions and Z=74. L_I theoretical curve shown for sake of comparison with L_{II} and L_{III} curves but all points are for L_{II} or L_{III} conversion lines.

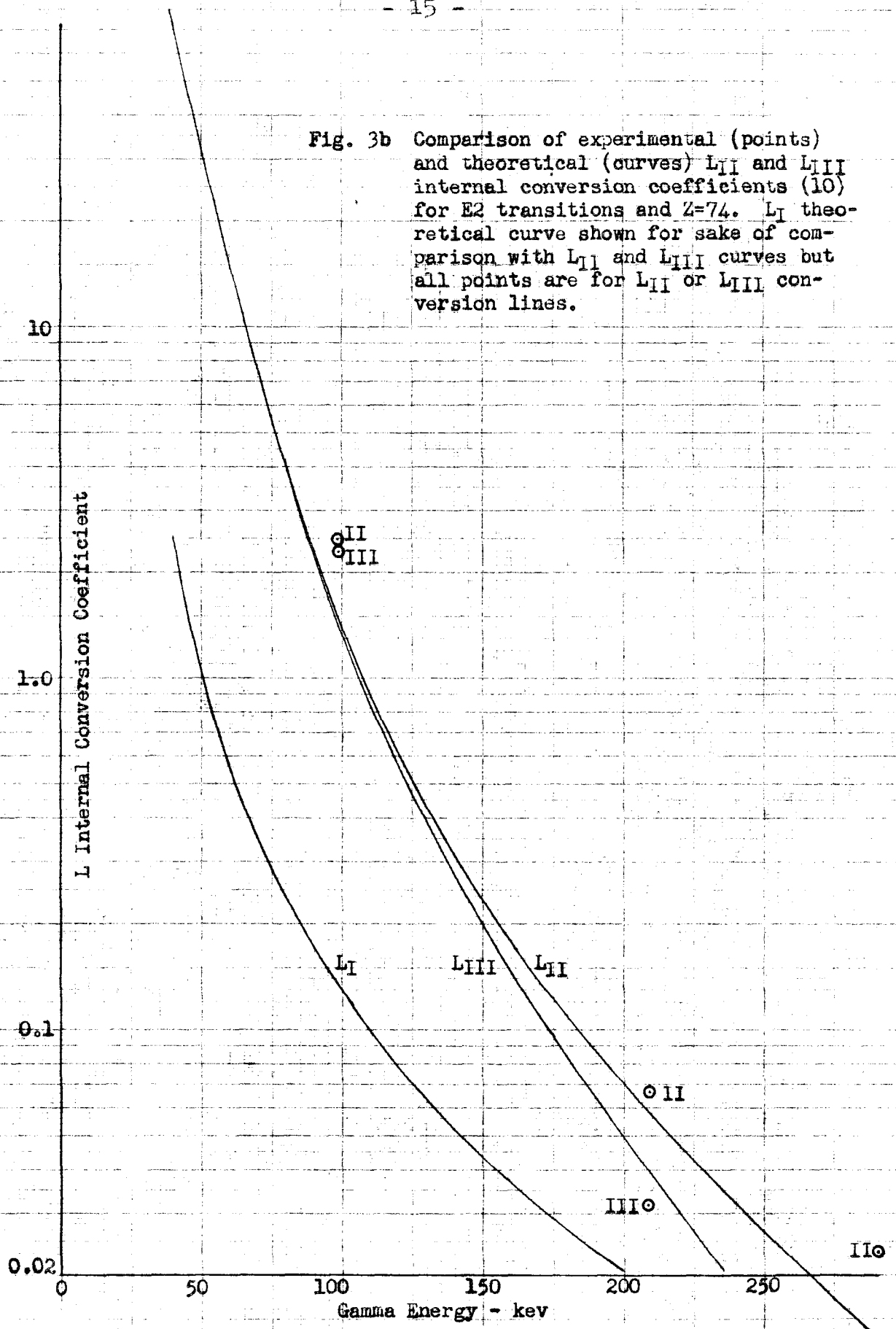

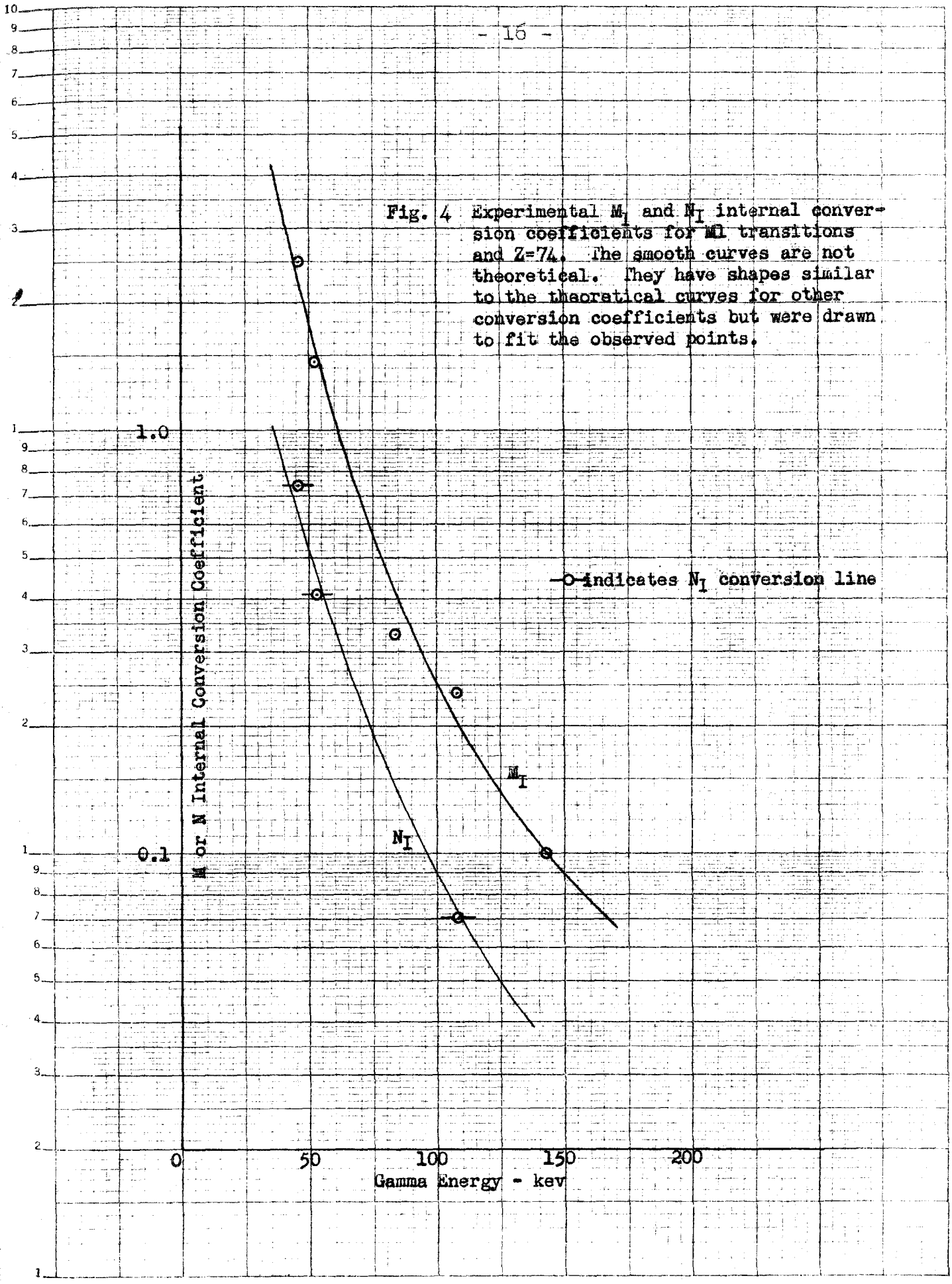

Fig. 4 Experimental M_I and N_I internal conversion coefficients for M1 transitions and Z=74. The smooth curves are not theoretical. They have shapes similar to the theoretical curves for other conversion coefficients but were drawn to fit the observed points.

III

TECHNIQUE AND ANALYSIS

General Procedure

Having both beta and gamma spectrometers available, it is important whenever possible to exploit their combined use in the study of a radioactive decay. Tantalum provided an excellent opportunity for so doing in that good sources (see Appendix I) could be prepared for both instruments. It is evident that the general coherence and completeness of the present results rest strongly on the combination of information from both instruments. In particular, the precision gamma energies enabled unambiguous identification of the conversion lines and only through the combination of gamma and conversion line intensities was it possible to calculate conversion coefficients (see TECHNIQUE AND ANALYSIS, Conversion Coefficients).

As indicated before, the tantalum sources used in these experiments were produced by irradiation in the Arco reactor. Only two such irradiations have been performed to date. The relatively short half life and complexity of the decay necessitated compromise operation designed to yield the best local data consistent with uniformly careful investigation over a wide spectral range. This meant the local data were not always the best possible. A future experiment concentrated on the weaker local details could certainly improve the present results.

Gamma Energies and their Role in Construction of the Level Scheme

The gamma energies were all obtained from the curved crystal gamma-ray diffraction spectrometer using techniques developed earlier and described elsewhere (5). They are based on calibration with the value 59.31 kev of the $W_{K\alpha_1}$ x-ray. They were obtained with a resolution, $\Delta E/E$, of $0.3E \cdot 10^{-2}$ percent, where E is the gamma energy in kev. (This dependence of resolution, $\Delta E/E$, proportional to energy E results from the fact that in the curved crystal gamma-ray diffraction spectrometer the minimum resolvable wavelength difference, $\Delta\lambda$, is practically constant throughout the entire spectral range). An uncertainty of 1/20 of the resolution or 10 volts, whichever is larger, was assigned to the absolute values.* Because of their precision, the gamma energies provided strong evidence on which to base the construction of the level scheme. Unfortunately, however, it is not possible to describe a straightforward, logical process by which the scheme was constructed from them. It developed piecemeal as more information became available and was not firm until the conversion data for the transitions was obtained. Using transition energies alone, the problem is quite similar to solving a jig-saw puzzle with no picture on it. Any additional information supplies the picture and bolsters one's

*The lower limit of 10 volts for the uncertainty of the absolute values of the gamma energies arises from possible uncertainty in the energy of the calibrating x-ray.

belief in the result.

The principal tool used to correlate the line energies was a table of sums of pairs of line energies and a list of equalities observed among them and between them and the line energies themselves. Table 4 gives a presentation of this information. Agreement within two parts in 5000 was used as a definition of equality. This small value is in general smaller than would be consistent with the uncertainties assigned to the gamma energies. The possibility of using so small a value in the definition of the equalities may indicate that the relative accuracy of the gamma energies is actually better than the uncertainty assigned to the absolute values.

In retrospect one may classify the equalities as being of three types. In the first type, the sum is the energy of a line or a missing line and there is likely to be more than one sum involved (see Table 4, equation (8) where five are involved). In the second type, the sum itself has no special meaning. Using the initial-final level designation for the transitions, one side of the latter type of equality is obtained from the other by exchanging the first or last letters in the designations of the two lines. It would be only by accident that more than two equal sums appeared in this type of equality. If one compiled differences rather than sums, the two types of equalities would just change places. The first type represents a double cascade with a cross-over or two or more double cascades in parallel. The second type

Table 4. Sums of Pairs of Gamma Energies (and single to pair and pair to pair equalities observed among them.)

Initial and final levels	Gamma Energy kev.				
IH	40.97				
BA	46.48	87.45			
CB	52.59	93.56	99.07C		
FE	82.92	123.89	129.40	135.51	
FD	84.70	125.67	131.18	137.29	167.62
CA	99.07	140.04	145.55	151.66	181.99
GD	101.94	142.91	148.42	154.53	184.86
	102.49	143.46	148.97(∝)	155.08	185.41
HG	103.14	144.11	149.62	155.73	186.06
DC	107.93	148.90(∝)	154.41	160.52	190.85
EC	109.73	150.70	156.21	162.32	192.65(43)
HF	120.38	161.35	166.86	172.97	203.30(a)
	142.25	183.22	188.73	194.84	225.17
IG	144.12	185.09	190.60	196.71	227.04
DB	160.53	201.50(β)	207.01D(38)	213.12	243.45
IF	161.36	202.33	207.84	213.95	244.28(3)
EB	162.33	203.30(a)	208.81E(39)	214.92	245.25(2)
FC	192.64	233.61	239.12	245.23(2)	275.56
HE	203.27	244.24(3)	249.75(b)	255.86	286.19
HD	205.06	246.03(6)	251.54	257.65	287.98(13)
EA	208.81	249.78(b)	255.29	261.40(9)	291.73F(45)
GC	209.87	250.84	256.35	262.46(1)	292.79
IE	244.26	285.23	290.74	296.85	327.18
ID	246.05	287.02	292.53	298.64	328.97(12)
FA	291.71	332.68	338.19	344.30	374.63
HC	313.03	354.00(8)	359.51	365.62(42)	395.95(11)
IC	354.04	395.01	400.52	406.63(37)	436.96(10)
HB	365.60	406.57(37)	412.08H(40)	418.19	448.52
IB	406.58	447.55	453.06I(41)	459.17	489.50
		40.97 IH	46.48 BA	52.59 CB	82.92 FE

NOTES:

1. Single to pair equalities denoted by underlining sum. Where a missing line is involved, underline is broken.
2. Pair to pair equalities of first type (see text) denoted by plain numbers in parenthesis after sum.
3. Pair to pair equalities of second type (see text) denoted by underlined numbers in parenthesis.
4. Accidental single to pair equalities have sum circled.
5. Accidental pair to pair equalities denoted by small arabic letter in parenthesis.
6. Sums equal to level energies are followed by capital letter designation of the level.
7. The pair to pair equalities denoted by (∝), (β) and (3′), (4′), (d), (ℓ) involve the 102.49 and 142.25 kev lines respectively, neither line appearing to be part of the main scheme (see text).

(α) 102.49 + BA = DC + IH
(β) 102.49 + CA = DB + IH
(3′) 142.25 + GD = (3)
(d) 142.25 + GC = DC + IE
(ℓ) 142.25 + EB = IG + DB
(4′) 142.25 + HD = (4)
} Note 7

183.77				
186.64	201.01			
187.19	201.56(β)	204.43		
187.84	202.21	205.08(44)	205.63	
192.63(43)	207.00D(38)	209.87	210.42	211.07
194.43	208.80E(39)	211.67	212.22	212.87
205.08(44)	219.45	222.32	222.87	223.52
226.95	241.32	244.19(3′)	244.74	245.39
228.82	243.19	246.06(6)	246.61	247.26
245.23(2)	259.60	262.47(1)	263.02	263.67
246.06(6)	260.43	263.30	263.85	264.50(22)
247.03	261.40(9)	264.27	264.82	265.47
277.34	291.71F(45)	294.58(16)	295.13	295.78
287.97(13)	302.34(i)	305.21	305.76	306.41(j)
289.76	304.13	307.00	307.55	308.20
293.51	307.88	310.75	311.30	311.95
294.57(16)	308.94G	311.81	312.36	313.01(46)
328.96(12)	343.33	346.20	346.75	347.40(4)
330.75	345.12	347.99	348.54	349.19(21)
376.41	390.78	393.65	394.20	394.85
397.73(15)	412.10H(40)	414.97(18)	415.52	416.17
438.74(14)	453.11I(41)	455.98(17)	456.53	457.18(20)
450.30	464.67	467.54	468.09	468.74
491.28	505.65(c)	508.52	509.07	509.72(19)
84.70 FD	99.07 CA	101.94 GD	102.49	103.14 HG

8. All 46 of the pair to pair equalities listed are not independent.

9. Equalities represent agreement within ± 2 parts in 5000.

(1) GC + CB = DB + GD = (GB)
(2) FC + CB = EB + FE = DB + FD = (FB
(3) HE + IH = IF + FE = IE
(4) IE + HG = HE + IG
(5) HB + DC = HC + DB
(6) HD + IH = IF + FD = IG + GD = ID
(7) IB + DC = IC + DB
(8) HC + IH = ID + DC = IE + EC =
GC + IG = FC + IF = IC
(9) EA + CB = EB + CA
(10) IC + FE = IE + FC

217.66				
228.31	230.11			
250.18	251.98	262.63		
252.05	253.85	264.50(22)	286.37	
268.46	270.26(23)	280.91	302.78	304.65(ℓ)
269.29	271.09	281.74	303.61	305.48
270.26(23)	272.06	282.71	304.58(ℓ)	306.45(j)
300.57	302.37(i)	313.02(46)	334.89	336.76
311.19	313.00(46)	323.64(k)	345.49	347.38(4)
312.99(46)	314.79	325.44	347.31(4′)	349.18(21)
316.74	318.54	329.19	351.06	352.93
317.80	319.60	330.25	352.12(d)	353.99(8)
352.19(d)	353.99(8)	364.64(30)	386.51	388.38
353.98(8)	355.78	366.43(29)	388.30	390.17
399.64	401.44(26)	412.09H(40)	433.96	435.83
420.96	422.76	433.40	455.28	457.15(20)
461.97	463.77	474.42(28)	496.29	498.16
473.53(5)	475.33(25)	485.98	507.85	509.72(19)
514.51(7)	516.31(24)	526.96(27)	548.83	550.70
107.93 DC	109.73 EC	120.38 HF	142.25	144.12 IG

(11) HC + FE = HE + FC
(12) ID + FE = IE + FD
(13) HD + FE = HE + FD
(14) IC + FD = ID + FC
(15) HC + FD = HD + FC
(16) GC + FD = FC + GD
(17) IC + GB = GC + ID
(18) HC + GD = HD + GC
(19) IB + HG = HB + IG
(20) IC + HG = HC + IG
(21) ID + HG = HD + IG
(22) IF + HG = HF + IG
(23) EB + DC = EC + DB
(24) IB + EC = EB + IC
(25) HB + EC = EB + HC

321.89				
322.86	323.69(k)			
353.17	354.00(8)	354.97		
363.80	364.62(30)	365.60(42)	395.91(11)	
365.59(42)	366.42(29)	367.39	397.70(15)	408.31(f)
369.34	370.17	371.14(e)	401.45(26)	412.08H(40)
370.40	371.23(e)	372.20	402.51	413.14
404.79	405.62	406.59(37)	436.90(10)	447.52
406.58(37)	407.41	408.38(f)	438.69(14)	449.32(33)
452.24	453.07I(41)	454.04(g)	484.35	494.98
473.56(5)	474.39(28)	475.36(25)	505.67(c)	516.30
514.57(7)	515.40	516.37(24)	546.68	557.31(32)
526.13	526.96(27)	527.93	558.24	568.87(h)
567.11	567.94	568.91(h)	599.22	609.85(31)
160.53	161.36	162.33	192.64	203.27
DB	IF	EB	FC	HE

(26) FA + EC = EA + FC
(27) IB + HF = HB + IF
(28) IC + HF = HC + IF
(29) ID + HF = HD + IF
(30) IE + HF = HE + IF
(31) IB + HE = HB + IE
(32) IC + HE = HC + IE
(33) ID + HE = IE + HD
(34) IB + HD = ID + HB
(35) IC + HD = ID + HC
(36) IB + HC = IC + HB
(37) HB + IH = IC + CB = ID + DB = IE + EB = IB
(38) DB + BA = DC + CA = D
(39) EB + BA = EC + CA = EA = E
(40) HB + BA = HC + CA = FA + HF = EA + HE = H
(41) IB + BA = IC + CA = FA + IF = IE + EA = I
(42) HC + CB = HD + DB = HE + EB = HB

413.87
414.93(18) 418.68
449.32(33) 453.07I(41) 454.13(g)
451.11 454.86 455.92(17) 490.31
496.77 500.52 501.58 535.97 537.76
518.09 521.84 522.90 557.29(32) 559.08(35)
559.10(35) 562.85 563.91 598.30 600.09
570.66 574.41 575.47 609.86(31) 611.65(34)
611.64(34) 615.39 616.45 650.84 652.63

205.06 208.81 209.87 244.26 246.05
HD EA GC IE ID

(43) EC + FE = DC + FD = FC
(44) HF + FD = HG + GD = HD
(45) EA + FE = FC + CA = FA
(46) IE + HG = HD + DC = FC + HF =
HE + EC = HC

604.74				
645.75	667.07			
657.31	678.63	719.64(36)		
698.29	719.61(36)	760.62	772.18	
291.71	313.03	354.04	365.60	406.58
FA	HC	IC	HB	IB

represents two pairs of lines, each pair having a common level and both interlocked around a third line. Finally, equalities of the third type are accidental ones representing impossible relationships. A priori, of course, one does not know the classification of the equalities except for some belonging to the first type, where the sums are equal to observed lines. Especially one does not know which are accidental, and, because of this, it is helpful to keep in mind certain statistical ideas when dealing with as large a number of lines as in the present case.

Given n numbers distributed randomly on a range 0 to R, the distribution of pair sums formed from them turns out to be

$$f(x) = \frac{n(n-1)}{2}\,\frac{1}{R^2}\begin{cases} x & \text{for } x < R \\ 2R-x & \text{for } x > R \end{cases} \qquad (1)$$

where x is the coordinate on the range. Defining "equality" to be within $(\Delta)x$, where Δ is a fraction, the probability of equality between a single number equal to x and a pair sum, or simply the probability of single-to-pair equality, is

$$P\left\{\text{single-to-pair equality}\right\} = (\Delta)n(n-1)\left(\frac{x}{R}\right)^2 \quad x<R \qquad (2)$$

and the expected number of such equalities over the whole range is

$$\left\langle\text{single-to-pair equalities}\right\rangle = \frac{(\Delta)n^2(n-1)}{3} \qquad (3)$$

Similarly the expected number of pair-to-pair equalities is

$$\langle \text{pair-to-pair equalities} \rangle = \frac{3}{4} (\Delta) \left[\frac{n(n-1)}{2} \right]^2 \qquad (4)$$

For $\Delta = 2/5000$ and n=29, these expected numbers are 3 and 49 respectively. In the present case, there turned out to be 53 single-to-pair equalities with 2 accidents and 101 pair-to-pair equalities with 23 accidents among them. (Equalities involving m equal sums have here been counted as m(m-1)/2 equalities.)

From this result it is clear that the probability of an equality of the second type being accidental is much greater than for a single-to-pair equality or one of the first type. Hence the sensible way to handle the equality information is to make tentative constructions based just on equalities known to be of the first type and to employ those of unknown type only as a check that relations predicted by the constructions actually exist. Proceeding in this fashion, one can without much difficulty arrive at the construction which makes use of a maximum number of the available equalities. There may, of course, be ambiguities in the final scheme. The present scheme, however, turned out to be unambiguous except for the possibility of complete inversion. To settle this ambiguity, other information is always needed. (see TECHNIQUE AND ANALYSIS, Spins).

Some of the accidental equalities, as shown in Table 4, involve the 102.49 and 142.25 kev lines neither of which it appears actually belong in the main scheme. Neither line has more than five percent decay fraction so there is little basis

other than energy data for determining their roles. No level arrangement incorporating one or both of these lines has been found which does not greatly increase the apparent number of accidental equalities, that is, without the ad hoc addition of levels and assumptions of additional β spectra for feeding them. It may be that these assumptions are necessary, but for the time being the 102.49 and 142.25 kev lines remain puzzling.

In addition to the obvious lower limit set by the highest energy transition, one may also establish a reasonable upper limit for the energy extension of tentative decay schemes from a knowledge of the end point energy of the β spectrum and an estimate of the Q value of the decay. For the odd-even Ta^{183} decay, going into a stable isotope, the Q value is expected to be on the order of 1 Mev, since for the nearby odd-odd decay of Ta^{182}, also going into a stable isotope, the Q is on the order of 2 Mev [1]. Hence, with a β spectrum end point of 615 kev, it would be unexpected if the proposed level scheme extended very much beyond the lower limit of 406 kev.

Conversion Line Energies

Gamma energies inferred from measured energies of their conversion lines by means of the absorption edges for the appropriate electronic shell are less accurate than those measured directly by the gamma spectrometer for several reasons. Some uncertainty is introduced through the values of the ab-

sorption edges and through the necessity to calibrate the beta spectrometer with an intermediate gamma line. Backgrounds are frequently high due to the presence of beta spectra. And, in the present case, the large number of conversion lines, larger than the number of gammas, required that less than a desirable length of time be spent on any particular line in order to cover them all in the time available. As a result the statistical errors were increased, especially for the weaker lines. Consequently, the conversion energies were used only as a means for identification of the conversion lines but were given no weight in the assignment of the gamma energies. The values actually measured are listed in Table 1 only as an indication of the validity of the identification and as reference for future work.

If one can assume the conversion electron lines have a momentum distribution narrow compared to the resolution of the instrument, then the shape of the characteristic line profiles obtained with the beta spectrometer can be expressed as a function of p/p_o where p is a variable proportional to momentum and p_o is a constant proportional to the momentum of the conversion line. In this case the profiles of two different lines normalized to the same peak and plotted on a logarithmic momentum scale will have exactly the same shape. This provides a convenient means for obtaining momentum ratios for conversion lines by determining the exact displacement on the logarithmic scale required to bring two profiles into exact register. If the energy loss suffered by electrons in

escaping from the source becomes sufficient, however, the electron line distribution may assume a width comparable to or exceeding the instrumental resolution and a shape which is not in general a function of p/p_o so that the logarithmic plotting technique becomes less effective.

Although the foregoing is, in principle, an ideal method for comparison of conversion line momenta, it was not actually used in the present experiments. The reason was that the data was taken by continuous chart recording and it was found that accuracy was lost in attempting to transfer the recorded data to a logarithmic scale. It was necessary to use the chart recording technique in order to reduce the time required for observation. Hence momentum ratios were obtained directly from the recorded data using the more common technique of comparison of fiducial points obtained by extrapolation of the high momentum side of the profiles into the background. With this spectrometer, the latter is a pretty good method since the characteristic line profile is almost triangular.

The momentum resolution obtained with the beta spectrometer using an internally converted source was 0.35% from 28.5 kev up. The energy precision claimed, namely 1 part in 1000 or 0.1 kev whichever is larger, therefore, never corresponds to less than 10% of the profile width.

Gamma Intensities

Relative intensities of the gamma lines were for the most part obtained from the gamma spectrometer, not without

extensive corrections to observed values in certain regions, however, so that their uncertainties are in general much greater than the statistical error. Apart from the gamma detecting device, the following energy dependent factors required corrections to the observed intensities:

1) absorption in the source and in the path to the detector, and

2) reflection coefficient of the crystal.

The source consisted of a cylindrical wire (see Appendix I) with the gamma rays emerging in a very small solid angle perpendicular to the cylinder axis. The path from source to detector was about 3 meters of air. Thus the correction for the first factor was easily computed, the principal uncertainty, a small one, entering through the absorption coefficient. Fig. 5 gives the internal absorption factor for a long cylinder of radius r and linear absorption coefficient μ. In the present case $2\mu r$ ranged from 0.08 at 400 kev to 4.3 at 40 kev so the maximum relative correction was about a factor four. The second factor was determined empirically by Lind, et al. [17] to vary like $1/E^2$, where E is the gamma energy, for E between 25 and 1400 kev. This result has been applied here.

The gamma detecting device was responsible for the major source of uncertainty in the gamma intensities. It consists of a NaI(Tl) scintillation crystal viewed by a single photomultiplier. The crystal is large so as to intercept the entire gamma beam with the result that as a scintillation spec-

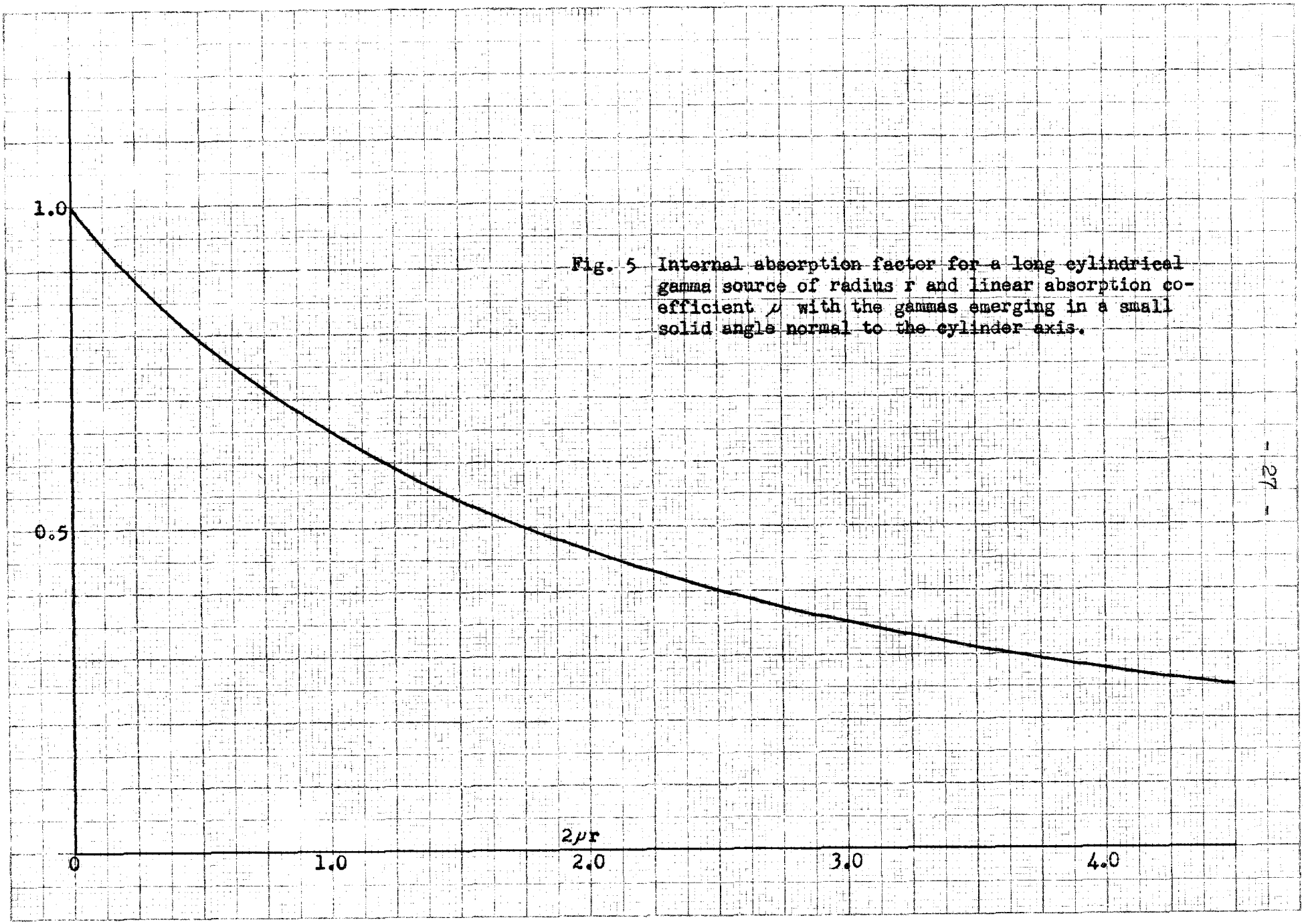

Fig. 5 Internal absorption factor for a long cylindrical gamma source of radius r and linear absorption coefficient μ with the gammas emerging in a small solid angle normal to the cylinder axis.

trometer at low energies the device has no resolution. The pulse height distribution is fairly well approximated as being linear, maximum at zero pulse height, zero for a height corresponding to the gamma energy minus a constant factor. This distribution passes a wide band discriminator with fixed high and low limits set for best signal-to-noise response, the lower discriminator being slightly above noise and the upper discriminator just above the peak pulses of the highest line energy. The upper discriminator has no effect but to eliminate high energy noise. The lower discriminator, however, removes an energy dependent fraction of the ideally countable distribution. On the basis of such a linear distribution and sharp discrimination the effect of the lower discriminator is accounted for by the factor,

$$\left(\frac{E-E_D-E_C}{E-E_C}\right)^2 \qquad (5)$$

where E is the gamma energy, E_D is the energy corresponding to the lower discriminator setting, and E_C is the constant difference between the end point of the pulse height distribution and E. From measured curves of counting rate versus lower discriminator setting, it was possible to estimate the value of the correction factor at the discriminator setting actually used for E equal to 52, 107, 161 and 246 kev. By adjusting E_D and E_C the above factor was fitted to these values and thereafter applied as a correction. At low energies its value was large amounting to 7 at 40 kev, 1.5 at

100 kev. The relatively large values of this and the $1/E^2$ factor account for the assignment of ±20% uncertainty for the intensities of gamma lines below 90 kev.

The beta spectrometer used with an externally converted source (see Appendix I) also provided relative gamma intensities for some of the lines. An externally converted beta source consists of a strong gamma source enclosed in a beta absorbing capsule with a thin layer of high Z material on the surface of the capsule acting as a photoelectric absorber and providing the actual beta source. The factors requiring correction of the observed intensities in this case are:

1) photoelectric cross section of the converter,
2) non-isotropic emission of electrons in the photo effect,
3) gamma absorption in the source and capsule, and
4) efficiency of the beta counter.

In general the corrections arising from these factors are smaller and can be determined more accurately than can those involved with the gamma spectrometer and as a result the intensities so obtained are more reliable. There were difficulties however in the case of Ta^{183}. Because of the large number of gamma lines and especially because of the presence of several strong lines on the order of 1 Mev belonging to Ta^{182}, the background due to Compton and photoelectrons from the main body of the source capsule was very high. The signal-to-noise ratios so obtained were much smaller than for the gamma spectrometer so that only the stronger lines could be observed

effectively. In addition the region below 50 kev was full of converted x-rays. As it turned out, it was possible to obtain reliable intensity measurements for only the five lines at 244, 246, 292, 313 and 354 kev and upper limits for the intensities of five other lines at 160, 161, 162, 205 and 209 kev. At these energies corrections for factors 3) and 4) above were negligible. Details of factors 1) and 2) are discussed in TECHNIQUE AND ANALYSIS, Conversion Coefficients where they also play an important role.

Conversion Line Intensities*

The beta counter efficiency was the only factor requiring correction of observed conversion line intensities. A Geiger counter having a mica beta window with an effective thickness of 1.1 mg/cm^2 was employed. The efficiency of such a counter is reduced at low energy. For the beta window described above the relative counter efficiency was about 30% at 28 kev compared to 100% for high energy electrons. A number of conversion lines appeared in the region between 28 and 50 kev, as may be seen from Table 1, so it was important to know the counter efficiency.

To this end, a preliminary experiment was conducted. Using the same counter which was later employed in the Ta^{183} experiments, the well known 518 kev β spectrum of Cs^{137} was observed. The shape of the spectrum so observed was compared

*Unless the adjective external is explicitly stated a "conversion line" in this thesis is understood to imply internal conversion.

to a shape based on observations of the same spectrum by Osaba [11] who used a counter with a window capable of transmitting 3.5 kev electrons. At high energies both spectra, after application of the first forbidden $\Delta I=2$, yes correction factor [12], yielded straight Kurie plots so that, suitably normalized, their ratio in the low energy region gave the relative efficiency of the counter used in the Ta^{183} experiments.

Fig. 6 gives the reciprocal of counter efficiency versus beta energy, obtained in the foregoing manner, which was applied as a correction to observed conversion line intensities. Error in this factor could be caused by the effect of different sources used here and in Osaba's observations and by improper extrapolation of Osaba's Kurie plot which had the characteristic upward bend below 100 kev. These considerations account for the higher uncertainties assigned to the intensities of conversion lines below 50 kev.

Conversion Coefficients

Given a set of corrected relative intensities, I_γ and I_β, for the gamma and conversion lines respectively and correct identification of the conversion lines, the conversion coefficients are given by

$$\alpha = C\frac{I_\beta}{I_\gamma} \qquad (6)$$

where C is a constant for all lines and conversions. The value of C may be established by assuming a pure multipole

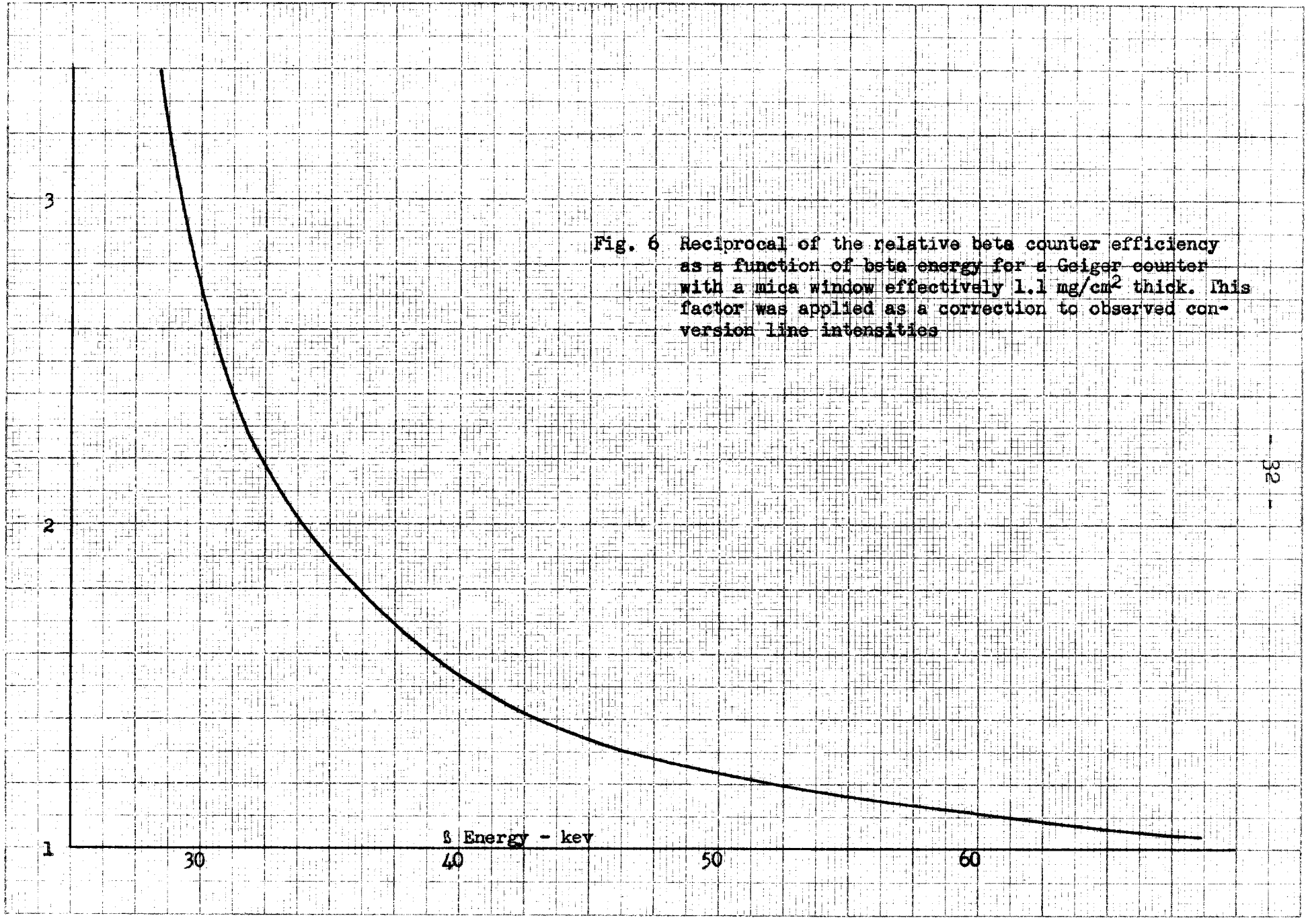

Fig. 6 Reciprocal of the relative beta counter efficiency as a function of beta energy for a Geiger counter with a mica window effectively 1.1 mg/cm^2 thick. This factor was applied as a correction to observed conversion line intensities

transition for some line which has conversion properties clearly associated with that multipole say, for example, on the basis of its K/L ratio and the L shell in which it is converted, and by setting α equal to the theoretical K-conversion coefficient [9]. If the gamma energy of the line is well above 150 kev, the theoretical K-conversion coefficient is presumably almost exact so that failure of this procedure to yield the correct value for C would be expected to arise only through the possibility of a mixture of multipoles in the transition. But in certain cases a limit may be established for the amount of error which could be caused by a mixed transition.

The absolute values of the conversion coefficients listed in Table 1 are based on the procedure outlined above for determining C. Their relative values, of course, do not depend on C. The 246.05 kev line, ID, has a K/L ratio of 5.4 and L-conversion takes place almost exclusively in the L_I shell. These facts indicate clearly that the transition is magnetic [10,13]. Both the K-conversion line and the gamma are among the stronger lines so it is highly improbable that the transition is anything but M1. The value of C obtained by making the assumption that the transition is pure M1 (and dependent, of course, on the scales of relative gamma and conversion line intensities) was 0.167. If the transition were E2, conversion in the L_{III} shell would give rise to a resolvable line which, from the theoretical conversion coef-

ficient for a transition of this energy (see conversion data for transition IE, Table 1) would have an expected intensity of 10.2 on the scale of relative conversion line intensities. In the region where the L_{III} conversion line might have appeared the minimum level of certain detection was 1.0. There was no L_{III} contribution with an intensity >1.5 so an upper limit of 15% was set on the possible amount of E2 admixture for the transition. With a ratio of 3.8:1 for the M1, E2 K-conversion coefficients, this implies that the value of C could be 10 or 11% lower than the value quoted above.

Another method was available to check the value of C, not as accurate in a fine sense as the foregoing method, but involving no special assumptions and accurate enough to eliminate the possibility of gross misjudgment in the assignment of M1 to the 246 kev line. The method involves calculation of the absolute value of an internal conversion coefficient from the intensities of both the internally and externally converted lines by knowing the conversion coefficient of the external converter and the ratio of strengths of the internally and externally converted sources. In this connection it is convenient to reexpress the internal conversion coefficient as

$$\alpha = \alpha_\gamma \frac{N_e}{N_i} \frac{I_\beta}{I_\gamma} \text{ (obs.)} \qquad (7)$$

where I_β is the corrected relative intensity of the internally converted line as before, I_γ(obs.) is the <u>observed</u> in-

tensity of the externally converted line expressed on the same relative scale as I_β (this is not the scale used for gamma intensities in Table 1), N_e/N_i is the ratio of the strength of the externally converted source to the strength of the internally converted source, and α_γ is the conversion coefficient of the external conversion assembly. $\frac{N_e}{N_i}$, I_β and I_γ (obs.) are measured quantities, N_e/N_i being measured by straightforward comparison of the two sources in the same geometry. The problem is to evaluate α_γ. It is implicit in the foregoing definitions that the transmission of the spectrometer is the same for the observation of I_β and I_γ (obs.). This condition was fulfilled.

α_γ may be expressed in the following manner:

$$\alpha_\gamma = FG\sigma_C T_C \frac{N_o}{A} \cdot 10^{-3} \qquad (8)$$

where N_o is Avogadro's number, A is the mass number of the converter material, T_C is the thickness of the converter in mg/cm^2, σ_C is the photoelectric cross section in cm^2 of the converter material, G is a dimensionless factor depending on the geometry of the gamma source and the converter, and F is another dimensionless factor correcting for the anisotropy of the photo effect. Defined in this way, α_γ is seen to contain the same energy dependent factors, F and σ_C, that were heretofore described as being responsible for corrections applied to the gamma intensities observed by external conversion. The application is the same here, only the association is different. It is noted that the presence of F in its defi-

nition means that α_γ is not just an energy dependent parameter for the converting assembly but also depends on the direction or directions of observation with respect to the converting assembly. Values of σ_C are available [16] and T_C is determined by knowledge of the mass and area of the converter. The problem remaining then, is to evaluate the factors F and G.

For a geometry in which the gamma source is a thin disc of radius R coaxial with and at a distance Z from a converter which is a thin disc of radius D, the factor G is given by

$$G = \frac{1}{\pi R^2} \int_0^R \int_0^D \int_0^\pi \frac{\rho r \, d\rho \, dr \, d\theta}{z^2 + \rho^2 + r^2 - 2\rho r \cos\theta} \qquad (9)$$

where r is a radial coordinate in the source disc, ρ is a radial coordinate in the converter disc, and θ is an angular coordinate about the axis of symmetry. Performing the integration and making a change of variable putting the integral in dimensionless form one obtains

$$G = \frac{1}{4} \int_0^1 \int_0^{(D/R)^2} \frac{dx \, dy}{\left\{ \left[(Z/R)^2 + x + y \right]^2 - 4xy \right\}^{1/2}} \qquad (10)$$

Though tedious, this integral may be evaluated with the result

$$G = \frac{1}{8}\left\{\left[\left(1-\left(\frac{D}{R}\right)^2\right)^2 + 2\left(1+\left(\frac{D}{R}\right)^2\right)\left(\frac{Z}{R}\right)^2 + \left(\frac{Z}{R}\right)^4\right]^{1/2} - \left(\frac{Z}{R}\right)^2 - \left(\frac{D}{R}\right)^2 - 1\right.$$

$$- 2\ln\frac{1}{2}\left\{\left[\left(1-\left(\frac{D}{R}\right)^2\right)^2 + 2\left(1+\left(\frac{D}{R}\right)^2\right)\left(\frac{Z}{R}\right)^2 + \left(\frac{Z}{R}\right)^4\right]^{1/2} - \left(\frac{Z}{R}\right)^2 - \left(\frac{D}{R}\right)^2 + 1\right\}$$

$$\left. + 2\left(\frac{D}{R}\right)^2 \ln\frac{1}{2}\left\{\left[\left(\left(\frac{R}{Z}\right)^2 - \left(\frac{D}{Z}\right)^2\right)^2 + 2\left(\left(\frac{R}{Z}\right)^2 + \left(\frac{D}{Z}\right)^2\right) + 1\right]^{1/2} + \left(\frac{R}{Z}\right)^2 - \left(\frac{D}{Z}\right)^2 + 1\right\}\right\} \qquad (11)$$

Fig. 7 shows the value of G as a function of Z/R for D/R=2. For the externally converted source actually used D/R was equal to 2, Z/R was equal to 1.1, so from Fig. 7 G was equal to 0.350.

In the beta spectrometer the conversion electrons actually observed are those emitted from the source in a small solid angle formed by a differential cone with a half angle of 45° coaxial with the disc forming the source. The anisotropy correction, F, may be defined as the ratio of the probability of emission of an electron into this solid angle compared to the same probability if the electrons were emitted from the source isotropically. The differential photo cross section is given by Heitler [19],

$$d\sigma_c = K\frac{\sin^2\theta}{(1-\beta\cos\theta)^4}\,d\Omega \qquad (12)$$

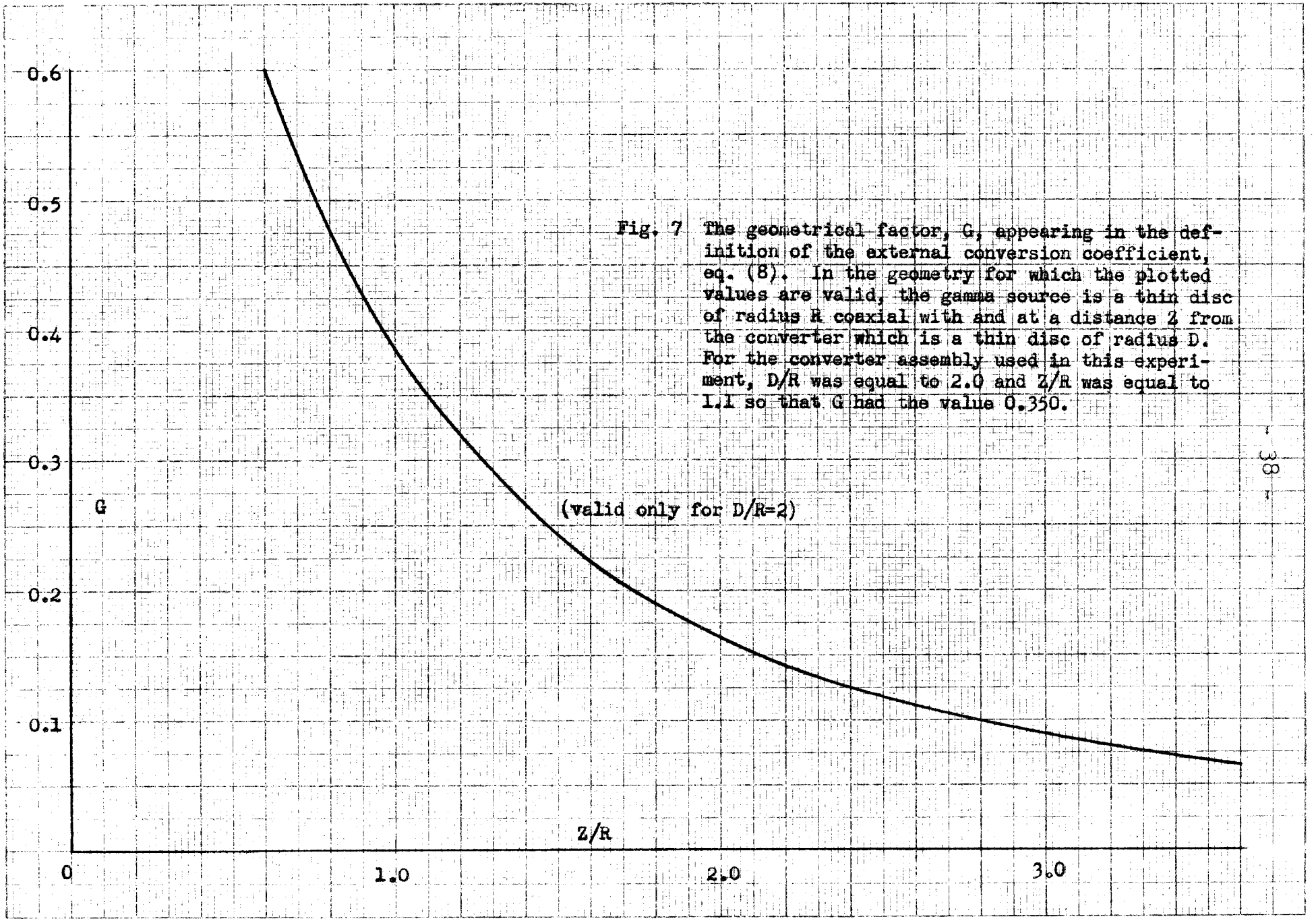

Fig. 7 The geometrical factor, G, appearing in the definition of the external conversion coefficient, eq. (8). In the geometry for which the plotted values are valid, the gamma source is a thin disc of radius R coaxial with and at a distance Z from the converter which is a thin disc of radius D. For the converter assembly used in this experiment, D/R was equal to 2.0 and Z/R was equal to 1.1 so that G had the value 0.350.

where K contains all but the angular dependence, β is the velocity of the ejected electron in units of the velocity of light, and θ is defined by

$$\vec{q} \cdot \vec{p} = \cos\theta \tag{13}$$

where $\vec{q}$ is a unit vector in the direction of the incident photon and $\vec{p}$ is a unit vector in the direction of the ejected electron. The total photo cross section is

$$\sigma_c = K \int \frac{\sin^2\theta}{(1-\beta\cos\theta)^4} d\Omega = \int K' d\Omega \tag{14}$$

which defines $K' d\Omega$ as the effective differential cross section were the photo effect isotropic. Finally F may be expressed as

$$F = \frac{K}{K'} \left\langle \frac{\sin^2\theta}{(1-\beta\cos\theta)^4} \right\rangle \tag{15}$$

where the average is over all directions in the small solid angle defined above and also over the directions of all the photons incident on the converter. Because of the latter average, F depends on the geometry of the gamma source and converter. Only the factor K/K' can be evaluated directly. It is given by

$$\frac{K}{K'} = \frac{\int d\Omega}{\int \frac{\sin^2\theta}{(1-\beta\cos\theta)^4} d\Omega} = \frac{3}{2}\left(1-\beta^2\right)^2 \tag{16}$$

Though straightforward, the averaging processes involve numerical integration. First, the average was evaluated for several angles of incidence of gammas arriving at the converter. The results are shown in Fig. 8 as a family of curves, each a function of β with the angle of incidence of the gamma with respect to the surface normal of the converter as a parameter. Then, interpolating from these curves, the second average over gammas incident from all parts of the gamma source was evaluated and this result, namely F, is also shown in Fig. 8. It is seen that F varies appreciably with energy so that it was important to know its value even for correction of relative gamma intensities.

The 354.04 kev gamma was slected for application of the foregoing calculations because its conversion lines, both the internally and externally converted K lines, were strong and completely in the clear and its energy was high enough so that the theoretical K-conversion coefficient would be expected to be good. The K-absorption edge for uranium is 115.3 kev so the electron energy of the externally converted K-line was 238.7 kev. For this energy the value of F obtained from Fig. 8 is 1.96. N_e/N_i had a measured value of 930. T_C was 0.5 mg/cm^2. The value of σ_C was 80 x 10^{-24}cm^2. The ratio of the intensities of the internal and external K-conversion lines, I_β/I_γ(obs.), was observed to be 2.1. On the basis of these values, the calculated value of the K-internal conversion coefficient for the 354.04 kev gamma turned out to be 0.135. The value obtained by the first

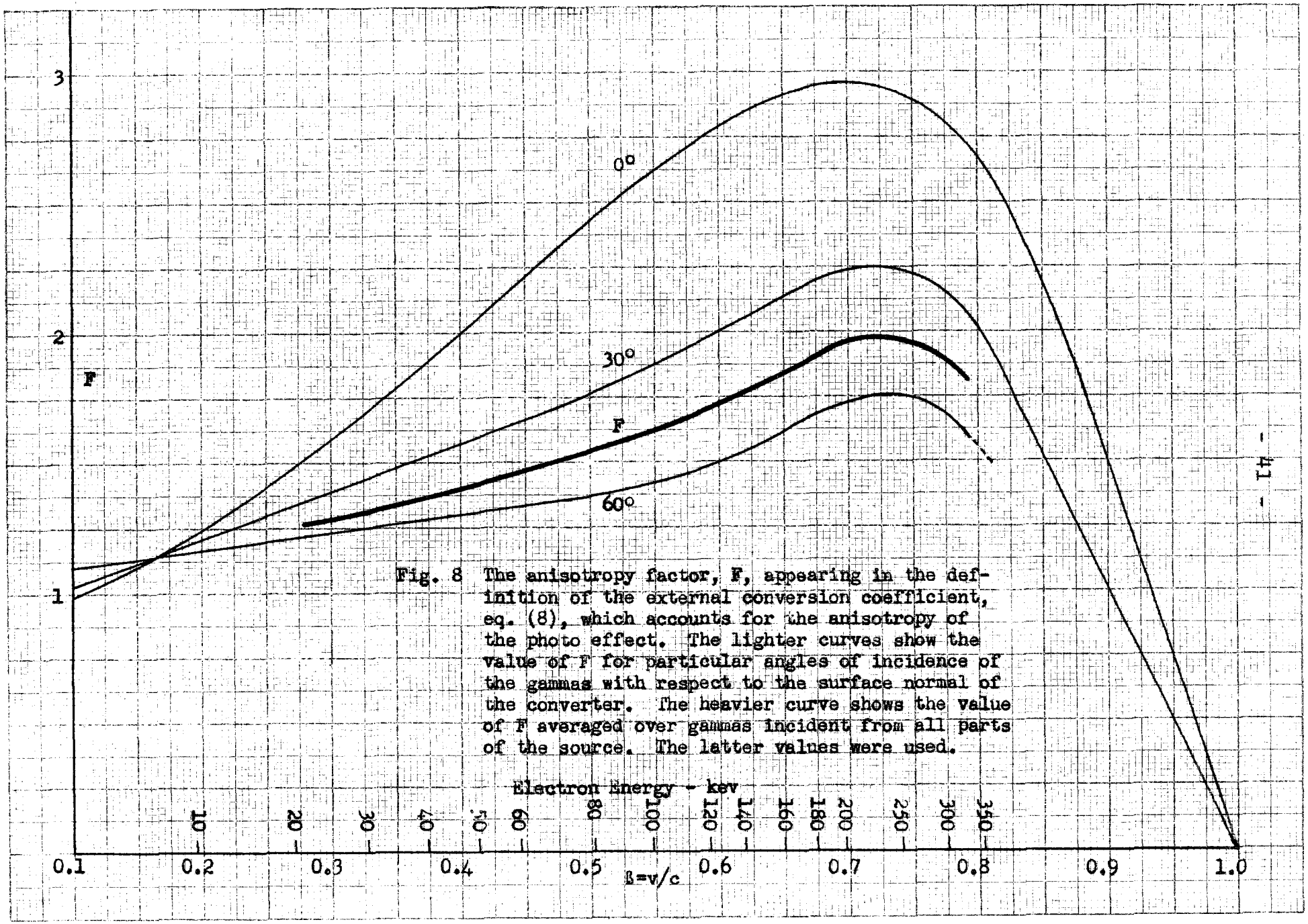

Fig. 8 The anisotropy factor, F, appearing in the definition of the external conversion coefficient, eq. (8), which accounts for the anisotropy of the photo effect. The lighter curves show the value of F for particular angles of incidence of the gammas with respect to the surface normal of the converter. The heavier curve shows the value of F averaged over gammas incident from all parts of the source. The latter values were used.

method (listed in Table 1) was 0.143. The theoretical M1 value is 0.145.

There are, however, many uncertainties involved in the calculation of α_γ. Its value in the preceding calculation would be assigned an uncertainty of about 20%. Also it was not possible to place as low a limit on possible E2 admixture in the 354 kev transition as in the case of the 246 kev transition owing both to the difficulty in resolving its L_{III}-conversion line and to lower expected values of its intensity. Therefore the above agreement cannot be taken too seriously. It is merely consistent with the assumption that the value used for C is not in gross error.

Decay Fractions

The corrected relative gamma intensities may be expressed as

$$I_\gamma = S\,\delta\,\frac{1}{1+\alpha_T}$$

so that

$$\delta = (1+\alpha_T)\,\frac{I_\gamma}{S}$$

where S is a constant for all lines, α_T is the total conversion coefficient and δ is the decay fraction for the line associated with I_γ. Relative decay fractions were calculated using this relation, first with an arbitrary value for S. Then the sum of the decay fractions into the ground state was normalized to 100 so that the results, shown in Table 1, give the decay fraction of each line expressed as a percentage of what goes into the ground state.

It is noted that in the low energy region where gamma intensities were more uncertain, δ depends mostly on conversion line intensities which were in general less uncertain. That is, α_T becomes much greater than unity at low energies so that

$$\delta = \frac{I_\gamma}{S}(1+\alpha_T) = \frac{I_\gamma}{S}\left[1 + C\left(\frac{I_{\beta_K}}{I_\gamma} + \frac{I_{\beta_{L_I}}}{I_\gamma} + \cdots\right)\right]$$

$$\approx \frac{C}{S}\left(I_{\beta_K} + I_{\beta_{L_I}} + \cdots\right) \qquad \alpha_T >> 1$$

At high energy, on the other hand, where $\alpha_T \ll 1$, δ depends almost entirely on I_γ. But here the I_γ are as good or better than the I_β so, in general, δ depends everywhere on the best intensity information. This is important because the agreement or disagreement of decay fractions into and out of the levels (see Table 3) is strong evidence for or against a proposed level scheme. Among the level schemes considered, none, other than the one proposed here, was free from gross disagreement in this connection.

Multipolarity Assignments and Parity of the Levels

The multipole assignments were made on the basis of comparison between observed and theoretical K and L-conversion coefficients. As may be seen by reference to the work of Rose et al. [9], all of the observed K-conversion coefficients differ by large factors from theoretical values for all but M1, E2 and E3 transitions. Values of E3 K-conversion coeffi-

cients fall in between those for E2 and M1. Even with large uncertainty in the observed coefficients, however, and possibilities of admixtures (especially E2 with M1), the fact that K/L ratios for magnetic transitions are much larger, on the whole, than those for electric transitions made it easy to rule out the E3 possibility for all those transitions appearing to be M1 from their K-conversion coefficients and for which the L conversion data were also available. Transitions DC, IG, IF, EB, HD, ID, HC and IC are examples of this situation as inspection of Table 1 reveals.

Furthermore, one can see from the theoretical L-conversion coefficients [1] plotted in Figs. 3a and 3b that M1 transitions convert almost entirely in the L_I shell and E2 transitions almost entirely in the L_{II} and L_{III} shells. The low energy transitions BA and CB are not converted in the K-shell, of course, but in both cases all three L-conversion lines were observed, the L_I lines predominating with conversion coefficients higher than but in rough agreement with theoretical M1 values. The experimental conversion coefficients would be expected to be higher than the theoretical values because the calculation of the latter neglected the effects of screening, important at low energy and especially in the L-shell. On this basis, these two transitions were interpreted as M1. (Transitions IH and FD were assigned M1 in the same way but are not essential to the ensuing argument).

From the decay scheme it may be verified that the ten

M1 transitions just considered form a network connecting all levels of the scheme. Therefore, from only this much of the data (but among the more reliable parts) one can conclude there is no parity change throughout the scheme. This conclusion eliminates any further possibility of E3 transitions being part of the scheme.

On this basis, other transitions for which no L-conversion data were available but which from their K-conversion coefficients appeared to be M1 were freely identified as such. The same idea applied in the interpretation of the apparent E2 transitions. In these cases, however, there was also evidence of predominant L_{II} or L_{III} shell conversion with coefficients consistent with theoretical E2 values. Transition IE, 244.26 kev, was an exception, its L-conversion lines being unresolved with the large L_I line of transition ID, 246.05 kev (see notes o and p, Table 1) so that its E2 assignment could be based only on the K-conversion coefficient.

Only the 102.49 kev transition was assigned other than M1 or E2 multipolarity. This line, as discussed earlier, does not appear to be part of the main scheme. Its large K-conversion coefficient is consistent with theoretical values for an M2 or E4 transition. Its K/L ratio equal to 5.5, however, indicates a magnetic transition so it was assigned M2. From this result, one would again conclude the line was not a part of the main scheme because M2 requires parity change.

For those transitions where the multipolarity has been inferred from the decay scheme, there were insufficient con-

version data to make an assignment. The inferred multipolarities are consistent, however, in the sense that they resulted in the prediction of no conversion lines with intensities sufficient for observation, or else observable lines so predicted were unresolved with much larger lines so that their existence could not be verified.

It should be mentioned that the theoretical K-conversion coefficients below 150 kev were extrapolated graphically from the actual calculations so that low energy portions of the theoretical curves shown in Fig. 2 cannot be expected to represent exact values even apart from the neglected effect of screening.

Spins

The assignments of spins to the various levels was based on the assumption that a transition will occur via the lowest possible multipole order. With this in mind, one can easily verify that starting at the bottom of the scheme with the known ground state spin, 1/2, and proceeding upward considering all alternatives, the spin assignments shown represent the only assignments satisfying all the observed spin changes.

The existence of such a set of spin assignments provides the only real evidence for the proposed orientation of the decay scheme. That is, if one turns the decay scheme over and attempts the same process of assigning spins, it is quickly found that no solution exists. If one believes the multipole assignments, this is good reason for orienting the

scheme as shown. The uniqueness of the spin assignments strengthens the argument.

The Continuous β Spectrum

Because of energy losses in the source, backscattering and scattering from appurtenances along the electron trajectories in a beta spectrometer, any conversion line gives rise to a certain amount of continuous background. With a large number of conversion lines, more or less uniformly distributed over a wide energy range as in these experiments, the continuous background due to the lines is appreciable compared to the continuous β spectrum. For this reason, it was not possible to observe the shape of the β spectrum so that only the ft value is available as an indication of the forbiddenness of the β decay. Furthermore, no useful limit could be set on the existence of β spectra with end points lower than that of the main transition, namely 615 kev.

It was possible, however, in view of the absence of strong conversion lines above 615 kev (there were a few around 1 Mev belonging to Ta^{182}) to place an upper limit of 5% on the relative amount of any β transitions with end points higher than 615 kev. This observation is consistent with the general agreement of decay fractions into and out of the various levels as shown in Table 3.

IV

DISCUSSION OF RESULTS

It is interesting to compare the behavior of W^{183} observed here as a result of excitation by the β^- decay of Ta^{183} with that of W^{183} excited by ϵ capture in Re^{183} and of the similar odd-even, odd neutron nuclei W^{185} and Hf^{179} excited respectively by β^- decay of Ta^{185} and ϵ capture in Ta^{179} (18).

The ϵ capture of Re^{183} gives rise to a complex gamma spectrum in W^{183} with the apparent existence of an isomeric state 80 kev above the ground state having a probable spin and parity of 7/2+. The present results indicate the existence of a 3/2-state only 46 kev above the ground state in W^{183}. From this one would suspect the possibility of an M2 transition between the 80 kev, 7/2+ state and the 46 kev, 3/2- state. It is surprising that the 7/2+ to ground state, E3 isomeric transition observed following the Re^{183} decay can compete if the M2 possibility actually exists.

The β^- decay of Ta^{185} goes into an isomeric state in W^{185} 75 kev above the ground state which deexcites to the ground state with a half life compatible with either an E3 or M3 transition. By similarity to the W^{183} nucleus, however, this state is presumed to be 7/2+. But also the ground state of Ta^{185} (odd proton) would be expected to be the same as Ta^{183}. So it is surprising that Ta^{183} would reject the possibility of a similar allowed β^- decay to the analogous

isomeric state in W^{183}, mentioned above, in favor of an apparently first forbidden decay into a higher level as observed here.

Hf^{179}, differing from W^{183} by only two protons and two neutrons, might be expected to have a level structure resembling that of W^{183}. The ϵ capture of Ta^{179} leading into Hf^{179}, however, gives rise to the scheme shown in Fig. 9. The levels appearing there are in themselves similar to levels E and G observed in W^{183}, both as to energy and spin and parity (see Fig. 1). But why the 9/2- level deexcites by an M3 transition with the apparent possibility of more favorable routes indicated by the level system of W^{183} is not clear.

Leaving the comparisons now and considering the decay scheme of W^{183} by itself, one observes that the absence of parity change throughout and of any state with spin 11/2 is in accord with shell theory. But from the existence of several transitions violating single particle selection rules (the ℓ-forbidden M1 transitions, CB, FE, EC, HG, IG and GD) and of E2 transitions competing successfully with M1, it is evident that the scheme is not in accord with the idea that the levels, (not all of them at least) represent ground states of single particle configurations of the shell model in this region.

The introduction of mixed configurations or many particle configurations would in general remove the ℓ-forbiddeness of the transitions just mentioned, but it is probably not possible,

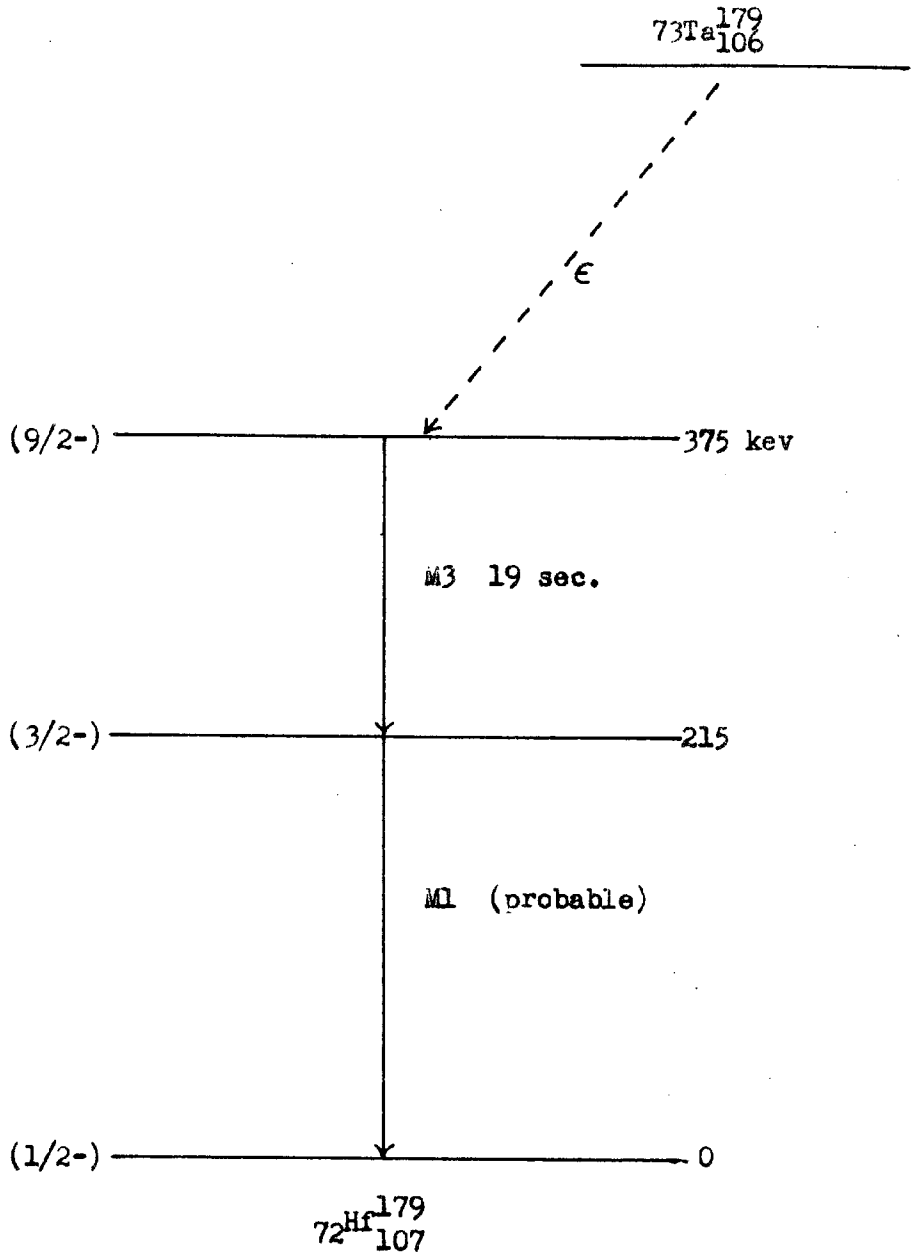

Fig. 9 Levels and transitions excited in Hf^{179} by electron capture in Ta^{179} (18).

without consideration of collective motion of all the nucleons, to account for quadrupole moments large enough to permit successful E2, M1 competition. The Bohr-Mottelson theory [20,21] seems to provide a logical mechanism for mixing states and for the production of large quadrupole moments greatly enhancing E2 transition probabilities without affecting those for M1 transitions. That is, the picture of the nucleus consisting of one or a few particles outside closed shells moving in the field of a deformable core formed by the bulk of the necleons in closed shells, includes the possibilities of coupling between the single particle configurations and the core and between single particle configurations through their mutual coupling to the core. The latter coupling can result in mixtures of states and many particle configurations different from those of the pure shell model while the particle-to-core coupling gives rise to families of states connected with rotational and vibrational components of surface oscillations of the core, each family associated with some single or many particle configuration.

It is possible that some of the levels observed in W^{183} fit into this picture. For example, it is tempting to regard the sequence of levels A, B, C, D and G, deexciting through a series of double M1 cascades, each with an E2 crossover, as a rotational family belonging to the ground state configuration. The energies of the levels are not those expected, however, if the ground state is assumed to be a single particle $p_{1/2}$ configuration. For such a configuration there is no

coupling to the surface oscillations of the core so that the 3/2, 5/2 and 7/2, 9/2 levels should be degenerate. One could conclude, therefore, that the ground state must be more complicated consisting, perhaps, of a three particle configuration or a mixture of single particle configurations. Furthermore, if this series of levels were really a rotational group, one would expect an 11/2- state somewhere above the 9/2 level. This would be in discord with shell theory. Such a state, if it exists, would probably be above the top of the present level scheme. If the ground state of Ta^{183} is 7/2+, it would require a $\Delta I=2$, yes or unique first forbidden β transition to excite the 11/2- state. Such a transition would be expected to be considerably slower than the $\Delta I=1$, yes transition which apparently does occur and for this reason the 11/2- state might not be excited appreciably.

Although such detail is, for the time being, just conjecture, the observation of enhanced E2 transition probabilities does represent strong evidence for participation of the core in the formation of at least some of the low-lying states of W^{183}.

APPENDIX I

SOURCES FOR THE GAMMA AND BETA SPECTROMETERS

As mentioned earlier, the Ta ^{183} used in this experiment was obtained from stable Ta^{181} by a double neutron capture.* For such a process, starting with a population N_1, of Ta^{181}, the populations N_2 and N_3 of Ta^{182} and Ta^{183} respectively after irradiation in a neutron flux ψ for a time t turn out to be given by

$$\frac{N_2}{N_1} = \frac{\sigma_1 \psi}{\lambda_2 + \sigma_2 \psi}\left[1 - e^{-(\lambda_2 + \sigma_2 \psi)t}\right] \qquad (A1)$$

$$\frac{N_3}{N_1} = \frac{\sigma_1 \sigma_2 \psi^2}{\lambda_3(\lambda_2 + \sigma_2 \psi)}\left\{1 - e^{-\lambda_3 t} - \lambda_3 t e^{-\frac{1}{2}(\lambda_3 + \lambda_2 + \sigma_2 \psi)t}\left[\frac{\sinh \frac{1}{2}(\lambda_3 - \lambda_2 - \sigma_2 \psi)t}{\frac{1}{2}(\lambda_3 - \lambda_2 - \sigma_2 \psi)t}\right]\right\} \qquad (A2)$$

where the only approximation is the assumption that N_1 is constant. σ_1 and σ_2 are the thermal neutron cross sections of Ta^{181} and Ta^{182} respectively and λ_2 and λ_3 are the decay constants of Ta^{182} and Ta^{183} respectively. The ratio of populations of Ta^{183} and Ta^{182} is given by

$$\frac{N_3}{N_2} = \frac{\sigma_2 \psi}{\lambda_3}\left\{\frac{1 - e^{-\lambda_3 t} - \lambda_3 t e^{-\frac{1}{2}(\lambda_3 + \lambda_2 + \sigma_2 \psi)t}\left[\frac{\sinh \frac{1}{2}(\lambda_3 - \lambda_2 - \sigma_2 \psi)t}{\frac{1}{2}(\lambda_3 - \lambda_2 - \sigma_2 \psi)t}\right]}{1 - e^{-(\lambda_2 + \sigma_2 \psi)t}}\right\} \qquad (A3)$$

*Ta^{181} is the only stable isotope of tantalum. The metal is obtainable in essentially pure form, the only appreciable impurity being tungsten ($<<$ 1%).

$$\xrightarrow[t\to\infty]{} \frac{\sigma_2 \psi}{\lambda_3} \tag{A4}$$

$$\xrightarrow[t\to 0]{} \frac{1}{2}\sigma_2\psi\left(\frac{\lambda_3+\lambda_2+\sigma_2\psi}{\lambda_2+\sigma_2\psi}\right)t \tag{A5}$$

The ultimate activity ratio of Ta^{183} to Ta^{182} immediately after irradiation is just

$$\frac{N_3}{N_2}\frac{\lambda_3}{\lambda_2} = \frac{\sigma_2\psi}{\lambda_2} \tag{A6}$$

In the Arco reactor where irradiations for this experiment were performed, the neutron flux is on the order of 2.5×10^{14} neutrons/cm^2/sec. For 115 day Ta^{182}, $\lambda_2 = 7 \times 10^{-8}$ 1/sec. Using the lower limit for σ_2, namely 10^4 barns [7], the ultimate activity ratio given above is 35. This illustrates the importance of the high neutron flux. A reduction of ψ by a factor 100, as in many other reactors, would have made the experiment impossible. The rise of the activity ratio is roughly exponential so that as seen from the small t approximation, eq. (A5), the irradiation time required for the activity ratio of Ta^{183} to Ta^{182} to reach half its ultimate value, using $\lambda_3 = 1.6 \times 10^{-6}$ 1/sec., is

$$t_{1/2} \approx 1.4\,\frac{1}{\lambda_3}\,\frac{1}{1+\frac{\lambda_3}{\lambda_2+\sigma_2\psi}}$$

$$= 1.2\,\tau_{1/2}(Ta^{183})$$

or a little longer than the 5.2 day half life of Ta^{183}. In this experiment a nine day irradiation was secured which

yielded an actual initial activity ratio on the order of 25 to 30.

The source for the gamma spectrometer was a round tantalum wire 3 cm long, 0.028 cm diameter. After the nine day irradiation its activity was about 10 curies most of which was due to Ta^{183}.

The gamma source used for external conversion in the beta spectrometer was a tantalum disc 0.0025 cm thick, 0.1 cm diameter. The nine day irradiation produced an activity of about 100 millicuries in this disc.

The external conversion assembly is shown in Fig. A1. The converter itself was a disc of uranium 0.5 mg/cm^2 thick, 0.2 cm diameter. It was prepared by evaporation of uranium on a thin mica sheet and subsequent punching of the 0.2 cm disc from the sheet. The mica disc was cemented to the beta absorbing copper capsule with the uranium surface exposed. The cylindrical hole in the copper capsule was made to fit the gamma source disc closely and the aluminum plug pressed the gamma source disc firmly against the flat bottom of the hole so that the geometry of the source and converter was well defined (see TECHNIQUE AND ANALYSIS, Conversion Coefficients where details of this geometry were involved in the calculation of the absolute value of a conversion coefficient).

The best sources used for internal conversion in the beta spectrometer were prepared by solid evaporation of the irradiated tantalum on mica. A disc of tantalum, like the one described above, was heated in a tungsten cup to a temperature

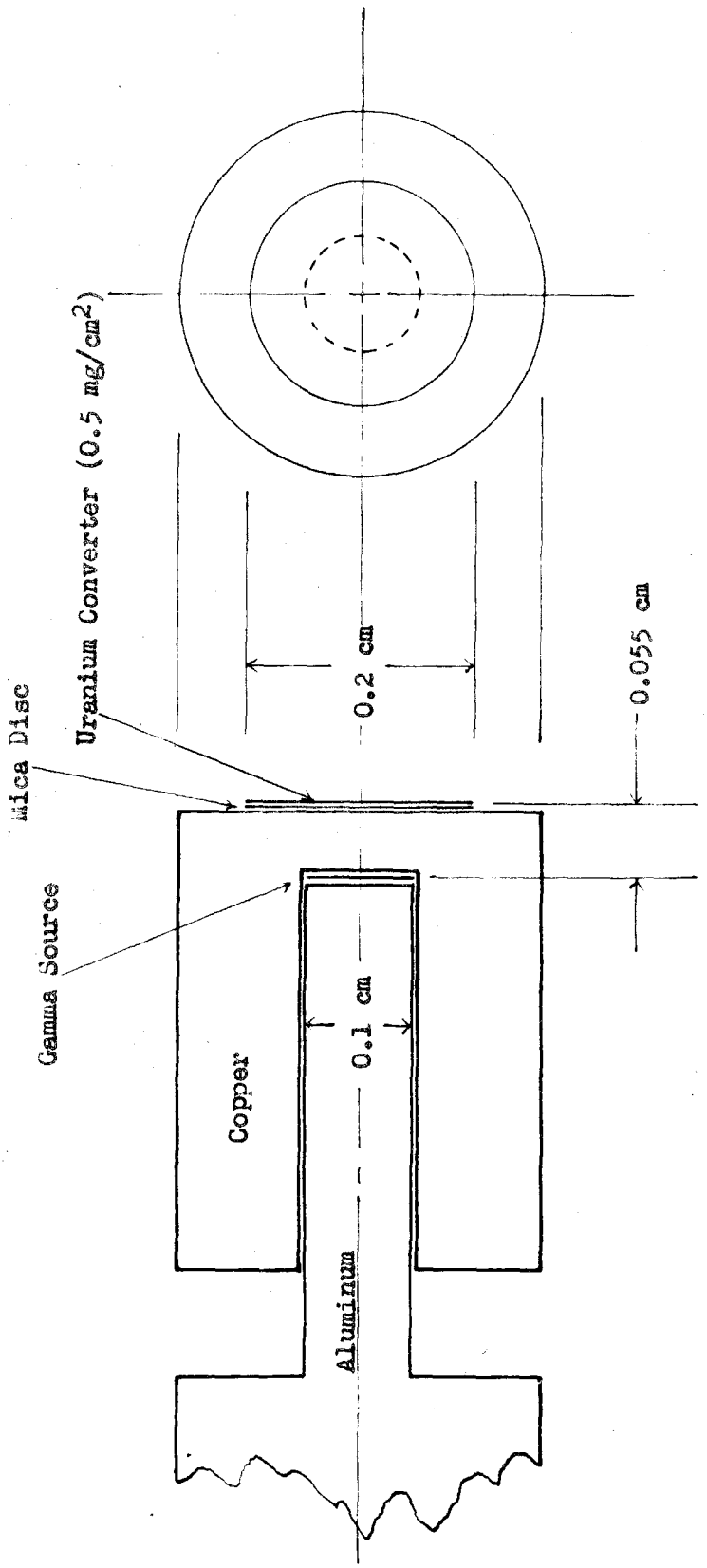

Fig. A1 External conversion assembly. See text for details of source and converter.

in the vicinity of its melting point, or about 3000° C. A thin sheet of mica was placed about 1 cm away from the tantalum. Heating for a few seconds sufficed to evaporate a very thin layer of tantalum on the mica. Subsequently, discs 0.1 cm diameter were punched from the mica, these serving as beta spectrometer sources. The activity of the discs so obtained was on the order of 100 microcuries so their thickness was on the order of 0.05 mg/cm^2. The latter is consistent with the observation that broadening of electron line distributions was small compared to about 0.7% energy resolution even at 28 kev electron energy.

APPENDIX II

THE L CONVERSION LINE GROUP OF THE 160.53, 161.36 AND 161.33 kev GAMMAS

As mentioned in note (ℓ) to Table 1, the L conversion lines of the transitions DB, IF and EB at 160.53, 161.36 and 162.33 kev gamma energy respectively formed a strong but unresolved group. The upper half of Fig. A2 shows the actual recorded profile for this group on a p/mc scale with relative intensities shown for the two unresolved peaks being measured on the same scale used in Table 1. Directly beneath the actual profile are shown the positions of fiducial points for all the possible L conversion lines of the group of gammas under consideration. (The fiducial point for a line is the intersection of the extrapolated high energy edge with the background.) No other conversion lines were expected to occur in this region. The multipolarities of these three transitions appeared to be E2, M1 and M1 respectively from their K-conversion coefficients. Fig. A3 shows a hypothetical profile constructed by assuming the existence of L_{II} and L_{III} lines for the E2 transition and L_I lines for the M1 transitions each line with an intensity equal to the value expected from theoretical L-conversion coefficients for the corresponding multipole. These L-conversion coefficients and the expected intensities of the various L lines are given in Table 1. The profiles used for the individual lines of the hypothetical composition are triangular in accordance with the

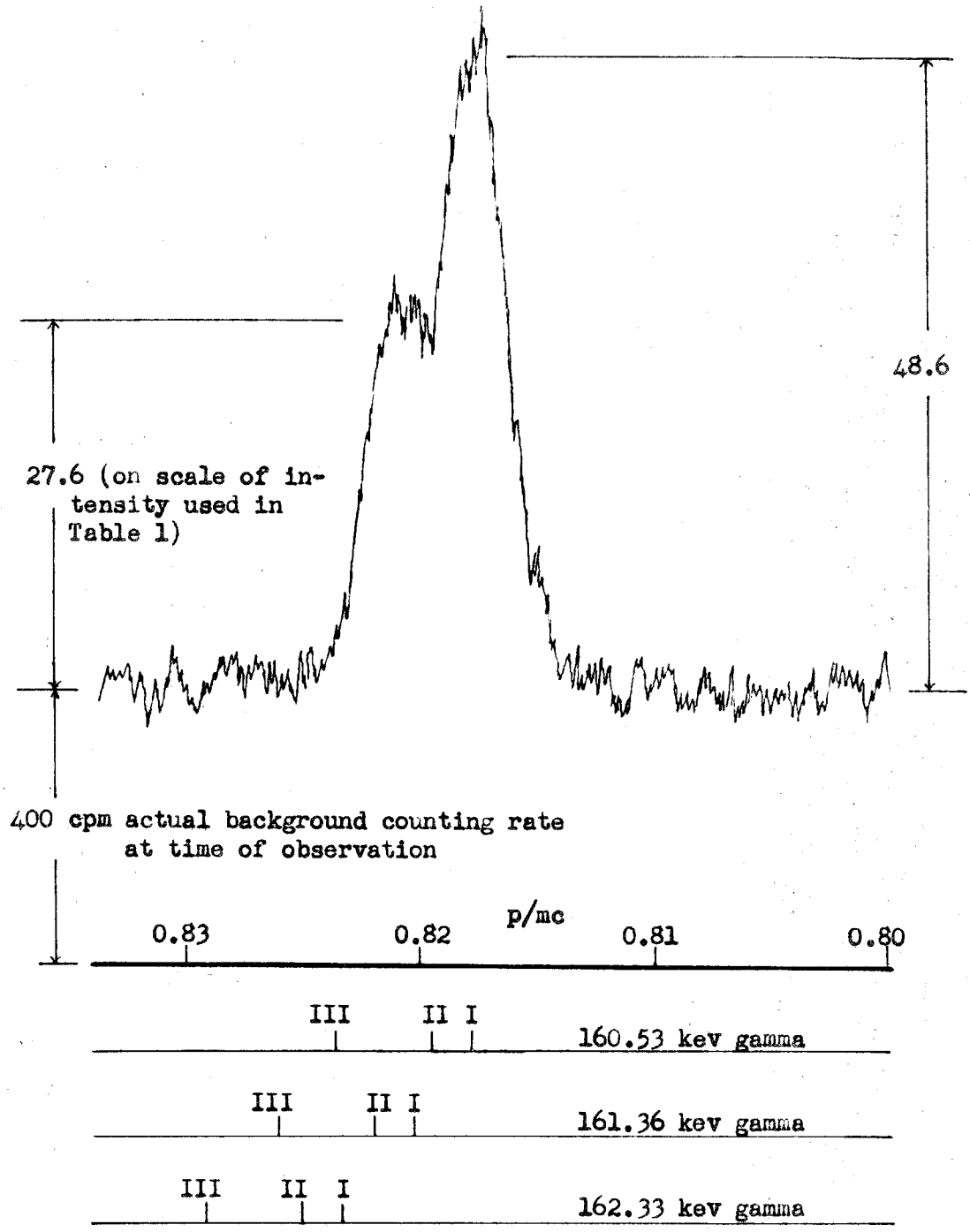

Fig A2 Above: actual profile of the unresolved group of L-conversion lines associated with transitions DB, IF and EB with 160.53, 161.36 and 162.33 kev gamma energy respectively. Below: calculated positions of fiducial points(see text) of all L-conversion lines of the three gammas mentioned above.

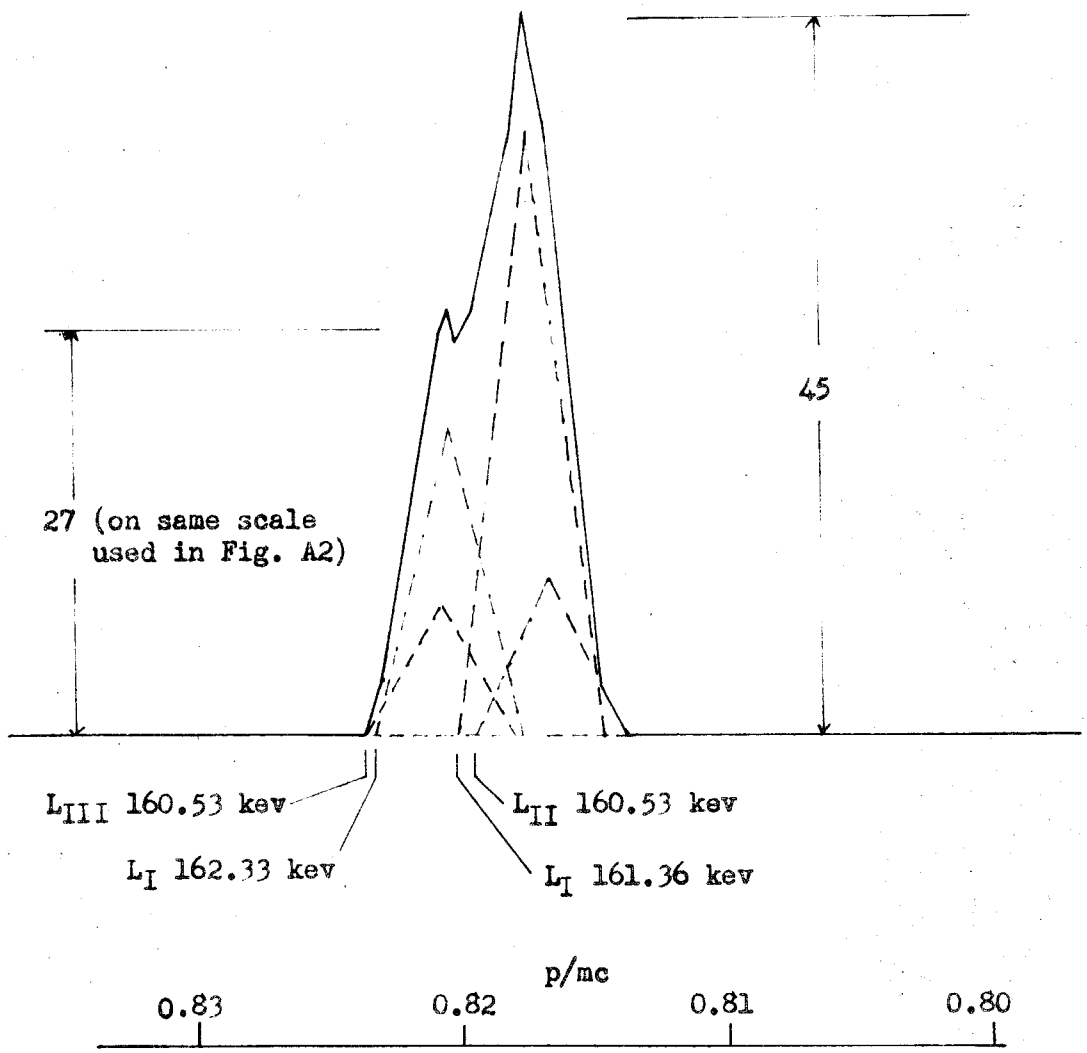

Fig. A3 Hypothetical profile of the unresolved group of L-conversion lines associated with the 160.53, 161.36 and 162.33 kev gamma lines constructed on the assumption that the multipolarities of these transitions were E2, M1 and M1 respectively. The intensities of the four L-conversion lines composing the profile were determined from theoretical L-conversion coefficients and are the expected values listed in Table 1 for those lines.

known characteristic profile of the instrument and their widths correspond to 0.35% momentum resolution determined from other resolved lines.

The hypothetical profile so constituted is seen to resemble the actual profile both as to shape and position on the p/mc scale. No other assumption as to multipolarities of the transitions involved was found to lead to hypothetical profiles resembling the actual one at all. This result is interpreted as a reasonable confirmation of the multipolarity assignments of these three transitions.

REFERENCES

1. Hollander, Perlman and Seaborg, Rev. Mod. Phys. 25, 469 (1953).
2. Butement, Nature 165, 149 (1950).
3. Wilkinson, MIT Report NP-1879 (Oct., 1950).
4. Moses and Martin, Phys. Rev. 84, 366 (1951).
5. Muller, Hoyt, Klein and DuMond, Phys. Rev. 88, 775 (1952).
6. Mihelich, Phys. Rev. 91, 427 (1953).
7. DuMond, Hoyt, Marmier and Murray, Phys. Rev. 92, 202 (1953).
8. DuMond, Kohl, Bogart, Muller and Wilts, ONR Special Technical Report No. 16 (March, 1952).
9. Rose, Goertzel, Spinrad, Harr and Strong, Phys. Rev. 83, 79 (1951).
10. Gellman, Griffith and Stanley, Phys. Rev. 85, 944 (1952).
11. Osaba, Phys. Rev. 76, 345 (1949).
12. Davidson, Phys. Rev. 82, 48 (1951).
13. Goldhaber and Sunyar, Phys. Rev. 82, 48 (1951).
14. Moszkowski, Phys. Rev. 82, 35 (1951).
15. Feenberg and Trigg, Rev. Mod. Phys. 22, 399 (1950).
16. White, NBS Report No. 1003 (May, 1952).
17. Lind, West and DuMond, Phys. Rev. 77, 475 (1950).
18. Goldhaber and Hill, Rev. Mod. Phys. 24, 179 (1952).
19. Heitler, The Quantum Theory of Radiation (Oxford University Press, London, 1950).
20. Bohr and Mottelson, Kgl. Dske. Vids. Selsk. Medd. 27, No. 16 (1953).

21. A. Bohr, Kgl. Dske. Vids. Selsk. Medd. 26, No. 14 (1952).

22. Hill, Church and Mihelich, Rev. Sci. Inst. 23, 524 (1952).